INTERNAL MEDICINE

□ CASE REPORT □

Peripartum Cardiomyopathy Presenting with Syncope due to Torsades de Pointes: a Case of Long QT Syndrome with a Novel KCNH2 Mutation

Orie Nishimoto[1], Morihiro Matsuda[1,3], Kei Nakamoto[1], Hirohiko Nishiyama[1], Kazuya Kuraoka[2], Kiyomi Taniyama[2,3], Ritsu Tamura[1], Wataru Shimizu[4] and Toshiharu Kawamoto[1]

Abstract

Peripartum cardiomyopathy (PPCM) is a cardiomyopathy of unknown cause that occurs in the peripartum period. We report a case of PPCM presenting with syncope 1 month after an uncomplicated delivery. Electrocardiography showed Torsades de pointes (TdP) and QT interval prolongation. Echocardiography showed left ventricular systolic dysfunction and endomyocardial biopsy showed myocyte degeneration and fibrosis. Administration of magnesium sulfate and temporary pacing eliminated recurrent TdP. Genetic analyses revealed that recurrent TdP occurred via electrolyte disturbance and cardiac failure due to PPCM on the basis of a novel mutation in KCNH2, a gene responsible for inherited type 2 long QT syndrome.

Key words: Torsades de pointes, long QT syndrome, peripartum cardiomyopathy

(Intern Med 51: 461-464, 2012)
(DOI: 10.2169/internalmedicine.51.5943)

Introduction

Peripartum cardiomyopathy (PPCM) is a disease of unknown cause that occurs from 1 month antepartum to 5 months postpartum in women without preexisting heart disease (1). In most cases, PPCM presents with signs of congestive heart failure caused by severe left ventricular (LV) systolic dysfunction. A few reported cases of PPCM have featured monomorphic ventricular tachycardia (VT) (2), but no cases have shown polymorphic VT.

Torsades de pointes (TdP), a polymorphic ventricular tachycardia associated with QT interval prolongation, is a life-threatening arrhythmia that can degenerate to fatal ventricular fibrillation. Acquired QT interval prolongation can occur upon exposure to environmental stressors such as particular classes of drugs, electrolyte disturbance, heart block, or heart failure (3). Moreover, in patients with drug-induced acquired long QT syndrome (LQTS), mutations have been identified in genes encoding cardiac ion channels, such as KCNQ1, KCNH2, and SCN5A, which have proven to be associated with congenital LQTS. Here, we report a rare case of PPCM presenting with recurrent syncope due to TdP resulting from a KCNH2 mutation.

Case Report

A 33-year-old woman was admitted to our hospital with repeated syncope and seizures 1 month after an uncomplicated delivery. She did not have a history of pregnancy-associated diseases, spontaneous abortion or epilepsy or any symptoms of infectious disease or heart failure during pregnancy or after delivery. Prior to this pregnancy she had a delivery without any complications, and had no family history

[1]Department of Cardiology, National Hospital Organization, Kure Medical Center and Chugoku Cancer Center, Japan, [2]Department of Diagnostic Pathology, National Hospital Organization, Kure Medical Center and Chugoku Cancer Center, Japan, [3]Institute for Clinical Research, National Hospital Organization, Kure Medical Center and Chugoku Cancer Center, Japan and [4]Division of Arrhythmia and Electrophysiology, Department of Cardiovascular Medicine, National Cerebral and Cardiovascular Center, Japan
Received for publication June 2, 2011; Accepted for publication September 11, 2011
Correspondence to Dr. Morihiro Matsuda, morihiro-m@kure-nh.go.jp

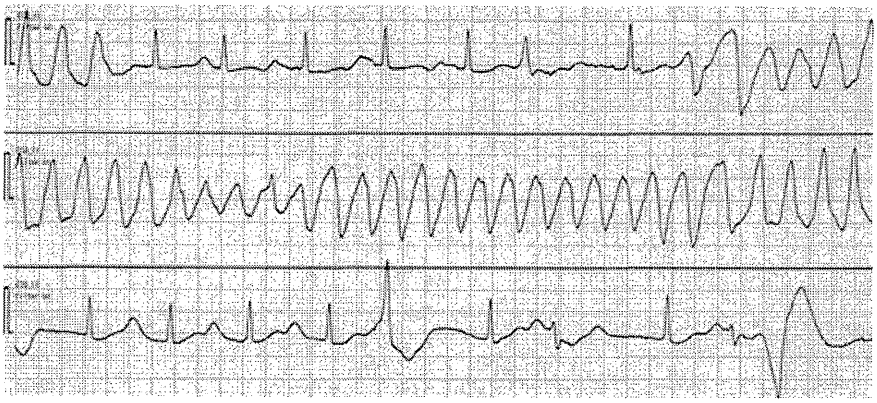

Figure 1. Electrocardiogram obtained at the time of syncope and seizure.

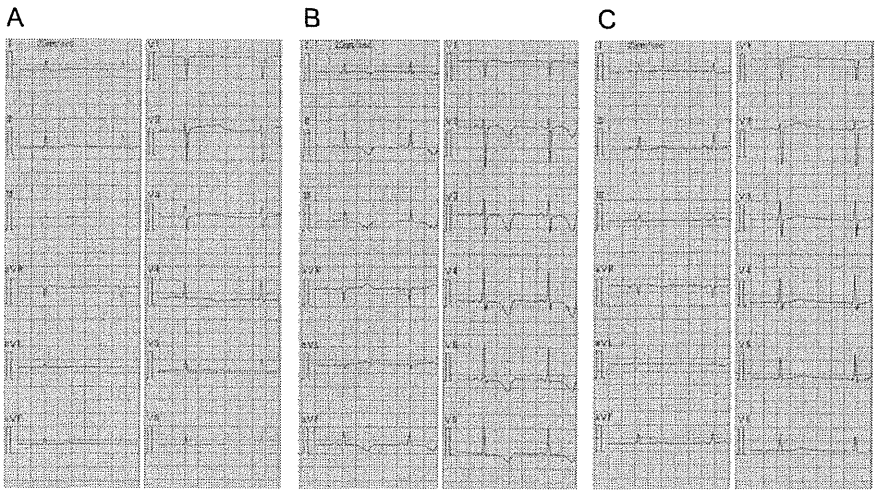

D

	Day 1	Day 8	Day 120
QTc (ms)	574	516	454
Blood Pressure (mmHg)	134/83	109/75	99/70
Heart Rate (bpm)	52	64	54
K (mEq/L)	3.4	4.4	4.2
Mg (mEq/L)	1.8	ND	ND

ND; not determined.

Figure 2. Changes in electrocardiographic findings. Electrocardiograms obtained on admission (A), at day 8 (B), and at day 120 (C). QTc, blood pressure, heart rate, and K and Mg levels on the indicated day (D).

of heart disease or sudden death. Syncope and seizures had occurred a day before admission and the next morning and evening prior to admission, and then she was taken to the emergency room in our hospital. She had taken no medicine before admission.

The patient was alert upon admission, and the following vital signs were noted: blood pressure, 134/83 mmHg; pulse rate, 50 bpm; and body temperature, 36.7℃. The patient's height and weight were 158 cm and 50 kg, respectively. Physical examination did not reveal any signs of heart failure or abnormal neurological findings. Electrocardiography (ECG) showed sinus bradycardia (50 bpm) and marked QT prolongation (QTc 574 ms) (Fig. 1, 2A). The chest X-ray image revealed a normal cardio-thoracic rate (48%) without pulmonary congestion or pleural effusion. Echocardiography showed impaired LV motion with mild hypokinesis at the base and severe hypokinesis at the apex. Laboratory data showed an elevated level of white blood cells (15,600/μL), mild elevation in the levels of brain natriuretic peptide (BNP) (123.1 pg/mL), hypokalemia (K levels, 3.4 mEq/L), and hypomagnesemia (Mg levels, 1.8 mEq/L), and normal serum levels of transaminases and creatinine. The levels of autoantibodies and viral antibodies were not significantly elevated, and the brain computed tomography image did not

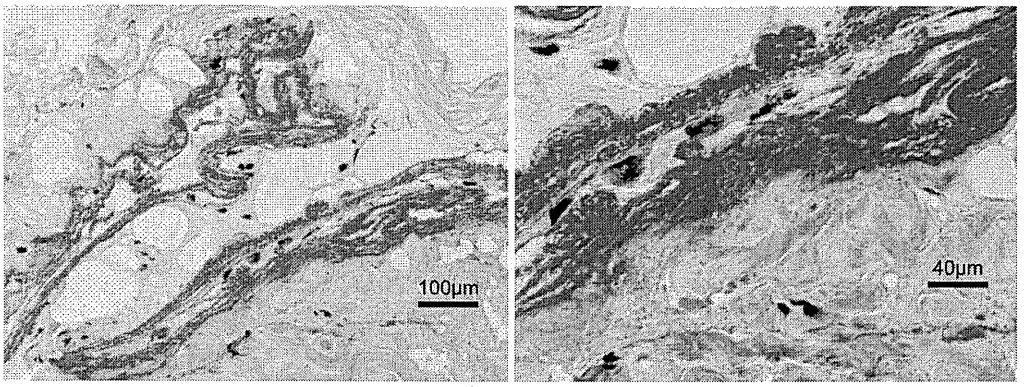

Figure 3. Endomyocardial biopsy revealing cardiomyopathy. Masson's trichrome stain.

indicate any abnormalities.

She presented with syncope and seizures immediately after admission, and the ECG monitor indicated TdP (Fig. 1) that spontaneously ceased in 10-20 s. In spite of intravenous administration of magnesium sulfate (166 mEq), TdP recurred twice within a few hours. Correction of hypokalemia and temporary pacing at a rate of 80 bpm effectively inhibited the repeated syncope caused by TdP. She was administered 2.5 mg/day of enalapril after admission. After day 11, TdP did not recur even after discontinuation of temporary pacing. The patient was discharged on day 23.

On day 3, left ventriculography showed mildly impaired LV wall motion with an ejection fraction of 43.6%, although coronary angiography revealed no significant stenosis in the coronary arteries. Endomyocardial biopsy of the right ventricle revealed myocytes degeneration and interstitial fibrosis (Fig. 3). Follow-up ECGs showed that the positive or flat T wave in the leads I, II, III, aVF, and V2-6 was inverted until day 8, and then gradually returned to the up-right or flat form on day 120 (Fig. 2A-C). Prolonged QTc was shortened to 516 ms on day 8 and 454 ms on day 120 (Fig. 2D). Follow-up echocardiography on day 120 showed that LV contraction was almost normal.

Genetic analyses of KCNQ1, KCNH2, and SCN5A in this patient revealed a novel mutation in the KCNH2 gene. This mutation involved an insertion of AGGC at exon 11 (c.2680_2681), leading to a frameshift from R894, which results in a C-terminal truncating mutation (p.R894fsX920) in KCNH2. This mutation was also identified in her mother and sister, resulting in border range QTc (mother, 467 ms; and sister, 461 ms) without any episodes of syncope. Her mother had experienced three uncomplicated deliveries and one spontaneous abortion, and her sister had not experienced pregnancy.

Discussion

PPCM is relatively rare, with a currently accepted estimate of an incidence of approximately 1 per 3,000 to 1 per 4,000 live births in the United States, but it can be life-threatening, with mortality rates between 18% and 56% (1). The present patient met the following 4 criteria for the diagnosis of PPCM, which was established by Demakis and Rahimtoola and others: 1) development of cardiomyopathy within 5 months of delivery, 2) absence of an identifiable cause of cardiomyopathy, 3) absence of recognizable heart disease before the last month of pregnancy, and 4) left ventricular systolic dysfunction with left ventricular ejection fraction (LVEF) of <45% (1, 4). Furthermore, histological investigation of the endomyocardial biopsy revealed myocyte degeneration and interstitial fibrosis, which may support the diagnosis of PPCM.

This PPCM patient showed recovery of ventricular function within 4 months after onset of syncope (5 months postpartum). Elkayam et al reported that recovery of LVEF (>50%) was observed in 54% of patients, and occurred within 6 months postpartum in most patients, which is distinct from other forms of non-ischemic cardiomyopathy. An improvement in LVEF at the last follow-up is significantly larger in women with an LVEF of >30% at time of diagnosis (5). For this reason, the present patient whose initial LVEF was 43.6% would be considered to be in a favorable position for spontaneous recovery. Similar to the medical management of patients with other forms of cardiomyopathy, ACE inhibitors and/or beta-blockers are commonly used for PPCM. Apart from the hemodynamic benefits of these classes of drugs, they may have the additional benefit of decreasing an overactive immune system, which plays a role in the basic pathophysiology of PPCM (6). Thus, the treatment of this patient with enalapril, an ACE inhibitor, from the first day after admission may have facilitated the improvement in PPCM.

The KCNH2 gene encodes the α-subunit of the voltage-gated potassium ion channel (Kv11.1, also called hERG), which plays a crucial role in ventricular repolarization. The role of KCNH2 is of particular pathophysiological importance, because mutations in this gene have been linked to the inherited type 2 long QT syndrome (LQT2) (3). We identified a novel KCNH2 gene mutation in the present patient and in 2 of her family members. This mutation was a 4-bp insertion leading to a C-terminal truncation of the hERG channel. Choe et al reported that functional assays

with 3 C-terminal truncating mutations in KCNH2 identified in the LQT2 families suggests an impaired ability of C-terminally truncated hERG protein to regulate channel activity in response to β-adrenergic stimulation (7). Based on their findings, we suspect that this novel mutation producing a truncated hERG protein at amino acid 920 should have a similar effect, although the functional effect of this mutation has not yet been clarified in vitro. Mild electrolyte abnormalities and cardiac failure due to PPCM led to marked QTc prolongation, and both the patient's QTc after recovery and those of her family members carrying this mutation were slightly prolonged (within border range), a finding that could be partly explained by this KCNH2 mutation. However, nevertheless, the patient's first delivery was uneventful, and her mother and sister were clinically unaffected by this mutation. Based on these facts, this mutation does not appear to have a strong impact on the phenotype of LQTS.

Women with LQT2, even without PPCM, are at increased risk for cardiac events during the postpartum period (8). However, it is difficult to predict cardiac events when such genetic mutations are not identified. Therefore, we recommend that the QT interval be measured in every pregnant woman, even those without preexisting cardiac diseases or a history of syncope to help prevent cardiac events, i.e., by avoiding hypokalemia and hypomagnesemia. In conclusion, we encountered a rare case of PPCM with recurrent syncope due to TdP. In this patient, inherited LQTS with KCNH2 mutation was unmasked via exposure to electrolyte disturbance and structural cardiac failure due to PPCM.

The authors state that they have no Conflict of Interest (COI).

References

1. Pearson GD, Veille JC, Rahimtoola S, et al. Peripartum cardiomyopathy: National Heart, Lung, and Blood Institute and Office of Rare Diseases (National Institutes of Health) workshop recommendations and review. JAMA **283**: 1183-1188, 2000.
2. Gemici G, Tezcan H, Fak AS, Oktay A. Peripartum cardiomyopathy presenting with repetitive monomorphic ventricular tachycardia. Pacing Clin Electrophysiol **27**: 557-558, 2004.
3. Roden DM, Viswanathan PC. Genetics of acquired long QT syndrome. J Clin Invest **115**: 2025-2032, 2005.
4. Demakis JG, Rahimtoola SH. Peripartum cardiomyopathy. Circulation **44**: 964-968, 1971.
5. Elkayam U, Akhter MW, Singh H, et al. Pregnancy-associated cardiomyopathy: clinical characteristics and a comparison between early and late presentation. Circulation **111**: 2050-2055, 2005.
6. Godsel LM, Leon JS, Engman DM. Angiotensin converting enzyme inhibitors and angiotensin II receptor antagonists in experimental myocarditis. Curr Pharm Des **9**: 723-735, 2003.
7. Choe CU, Schulze-Bahr E, Neu A, et al. C-terminal HERG (LQT 2) mutations disrupt IKr channel regulation through 14-3-3epsilon. Hum Mol Genet **15**: 2888-2902, 2006.
8. Seth R, Moss AJ, McNitt S, et al. Long QT syndrome and pregnancy. J Am Coll Cardiol **49**: 1092-1098, 2007.

A Connexin40 Mutation Associated With a Malignant Variant of Progressive Familial Heart Block Type I

Naomasa Makita, MD, PhD; Akiko Seki, MD, PhD; Naokata Sumitomo, MD, PhD; Halina Chkourko, MS; Shigetomo Fukuhara, PhD; Hiroshi Watanabe, MD, PhD; Wataru Shimizu, MD, PhD; Connie R. Bezzina, PhD; Can Hasdemir, MD; Hideo Mugishima, MD; Takeru Makiyama, MD, PhD; Alban Baruteau, MD; Estelle Baron, BS; Minoru Horie, MD, PhD; Nobuhisa Hagiwara, MD, PhD; Arthur A.M. Wilde, MD; Vincent Probst, MD, PhD; Hervé Le Marec, MD; Dan M. Roden, MD; Naoki Mochizuki, MD, PhD; Jean-Jacques Schott, PhD; Mario Delmar, MD, PhD

Background—Progressive familial heart block type I (PFHBI) is a hereditary arrhythmia characterized by progressive conduction disturbances in the His-Purkinje system. PFHBI has been linked to genes such as *SCN5A* that influence cardiac excitability but not to genes that influence cell-to-cell communication. Our goal was to explore whether nucleotide substitutions in genes coding for connexin proteins would associate with clinical cases of PFHBI and if so, to establish a genotype-cell phenotype correlation for that mutation.

Methods and Results—We screened 156 probands with PFHBI. In addition to 12 sodium channel mutations, we found a germ line *GJA5* (connexin40 [Cx40]) mutation (Q58L) in 1 family. Heterologous expression of Cx40-Q58L in connexin-deficient neuroblastoma cells resulted in marked reduction of junctional conductance (Cx40-wild type [WT], 22.2±1.7 nS, n=14; Cx40-Q58L, 0.56±0.34 nS, n=14; $P<0.001$) and diffuse localization of immunoreactive proteins in the vicinity of the plasma membrane without formation of gap junctions. Heteromeric cotransfection of Cx40-WT and Cx40-Q58L resulted in homogenous distribution of proteins in the plasma membrane rather than in membrane plaques in ≈50% of cells; well-defined gap junctions were observed in other cells. Junctional conductance values correlated with the distribution of gap junction plaques.

Conclusions—Mutation Cx40-Q58L impairs gap junction formation at cell-cell interfaces. This is the first demonstration of a germ line mutation in a connexin gene that associates with inherited ventricular arrhythmias and emphasizes the importance of Cx40 in normal propagation in the specialized conduction system. **(*Circ Arrhythm Electrophysiol.* 2012; 5:163-172.)**

Key Words: heart block ■ genes ■ ion channels ■ death sudden ■ gap junctions

Cardiac myocyte excitability in atria, His-Purkinje system, and ventricles is largely determined by the properties of voltage-gated sodium channels. Once activated, excitatory currents rapidly propagate to neighboring cells through low-resistance intercellular channels called gap junctions, which facilitate the synchronous contraction of the heart.[1,2] Loss of expression and function of cardiac gap junctions and sodium currents can severely impair action potential propagation, which sets the stage for life-threatening arrhythmias.[1,2] Although multiple mutations in genes coding for components of the voltage-gated sodium channel complex have been previously described in relation to arrhythmias and sudden death in young persons[3] and connexin40 (Cx40) mutations have been implicated in atrial fibrillation,[4,5] no study has identified an

Clinical Perspective on p 172

Received September 24, 2011; accepted January 9, 2012.

From the Department of Molecular Pathophysiology, Graduate School of Biomedical Sciences, Nagasaki University, Nagasaki, Japan (N. Makita); Cardiology, Tokyo Women's Medical University, Tokyo, Japan (A.S., N.H.); Pediatrics and Child Health, Nihon University School of Medicine, Tokyo, Japan (N.S., H.M.); Cardiology, New York University Medical School, New York, NY (H.C., M.D.); Cell Biology, National Cerebral and Cardiovascular Center Research Institute, Suita, Japan (S.F., N. Mochizuki); Cardiology, Niigata University Graduate School of Medical and Dental Sciences, Niigata, Japan (H.W.); Cardiology, National Cerebral and Cardiovascular Center, Suita, Japan (W.S.); Experimental Cardiology, Academic Medical Center, University of Amsterdam, Amsterdam, The Netherlands (C.R.B., A.A.M.W.); Cardiology, Ege University School of Medicine, Bornova, Izmir, Turkey (C.H.); Cardiovascular Medicine, Kyoto University Graduate School of Medicine, Kyoto, Japan (T.M.); l'institut du thorax, INSERM UMR915, Nantes, France (E.B., V.P., H.L., J.-J.S.); Cardiovascular Medicine, Shiga University of Medical Science, Otsu, Japan (M.H.); and Pharmacology and Medicine, Vanderbilt University, Nashville, TN (D.M.R.).

The online-only Data Supplement is available with this article at http://circep.ahajournals.org/lookup/suppl/doi:10.1161/CIRCEP.111.967604/-/DC1.

Correspondence to Naomasa Makita, MD, PhD, Department of Molecular Pathophysiology, Graduate School of Biomedical Sciences, Nagasaki University, 1-12-4 Sakamoto, 852-8523 Nagasaki, Japan. E-mail makitan@nagasaki-u.ac.jp

Circ Arrhythm Electrophysiol **is available at http://circep.ahajournals.org** **DOI: 10.1161/CIRCEP.111.967604**

association between germ line mutations in gap junction proteins and inherited ventricular arrhythmias in humans.

In this study, we investigated a group of patients with progressive familial heart block type I (PFHBI) (Online Mendelian Inheritance in Man 113900), also known as progressive cardiac conduction defect or Lenègre-Lev disease,[6,7] is a dominant inherited disorder of the His-Purkinje system. Affected individuals show electrocardiographic evidence of bundle branch disease (ie, right bundle branch block, left anterior or posterior hemiblock, complete heart block) with broad QRS complexes. The disease can progress from a normal ECG to right bundle branch block and from the latter to complete heart block. Affected individuals often present with family history of syncope, pacemaker implantation, and sudden death.[8] Although structural abnormalities have been invoked as a cause of the disease,[6,7] a number of patients present with normal cardiac structure and contractile function. Linkage analysis in a large South African PFHBI kindred[9] and a Lebanese kindred[10] mapped a causal locus on chromosome 19q13.3, and further work identified mutations in genes encoding for the transient receptor potential nonselective cation channel, subfamily M, member 4 (*TRPM4*) gene[11] at this locus. Haploinsufficiency of *SCN5A* and aging have been implicated in PFHBI,[8] and age-dependent manifestations of the disease have been recapitulated in mice.[12]

Here, we sought to expand on the association between PFHBI and mutations in genes relevant to action potential propagation; in particular, we assessed the possible association between nucleotide substitutions in connexin-coding genes and PFHBI. We evaluated 156 probands of diverse ethnic backgrounds from Asia, Europe, and North America given a clinical diagnosis of PFHBI. In addition to the sodium channel mutations previously reported,[13–15] we identified a germ line missense mutation in *GJA5* in a family with severe, early onset disease. This gene codes for the gap junction protein connexin40 (Cx40), which predominantly expresses in the atria and His-Purkinje system.[16] Heterologous expression experiments revealed that this novel mutation (Cx40-Q58L) significantly impaired the ability of Cx40 to form gap junction channels. Confocal microscopy showed that the Cx40-Q58L mutant but not the wild type (WT) failed to form plaques at sites of cell-cell apposition. Coexpression experiments indicated that the Cx40-WT protein provided only partial rescue of the Cx40-Q58L cellular phenotype. To our knowledge, this is the first description of a germ line mutation in a connexin gene associated with inherited ventricular arrhythmias. The results open the possibility of *GJA5* as a candidate gene for screening in patients with PFHB1, yet in the absence of further evidence, screening may be limited to the research environment rather than included as a part of the routine diagnostic examination.[17] The data also emphasize the importance of Cx40 in the maintenance of normal propagation in the specialized conduction system of the human heart.

Methods

Genetic Screening of PFHB1

Genomic screening by polymerase chain reaction and DNA sequencing was performed for *GJA5* (Cx40), *GJA1* (Cx43), *GJC1* (Cx45), *KCNQ1*, *KCNH2*, *SCN5A*, *KCNE1*, *KCNE2*, *KCNJ2*, *SCN1B*, *SCN4B*, *HCN4*. Primer information is provided in the online-only Data Supplement. All participating probands and family members gave written informed consent in accordance with standards (Declaration of Helsinki) and local ethics committees.

Plasmid Construction

A 1.1-kb Cx40-DNA fragment was subcloned into bicystronic plasmids pIRES2-EGFP and pIRES2-DsRED2. An EGFP or FLAG epitope was added at Cx40 C terminal to generate EGFP- or FLAG-tagged Cx40. Site-directed mutagenesis (Q58L) was performed with QuikChange. Primer information and additional details are provided in the online-only Data Supplement.

Cell Culture and Transfection

Constructs were introduced into connexin-deficient HeLa cells or mouse neuroblastoma (N2A) cells using Lipofectamine as per manufacturer's protocol.

Electrophysiology

Gap junction currents were recorded from transiently transfected N2A cell pairs using whole-cell double-patch clamp techniques as previously described.[18,19] Further details are provided in the online-only Data Supplement.

Immunocytochemistry and Western Blotting

HeLa cells, transfected with pEGFPN1-Cx40-WT, pCMV-FLAG-Cx40-Q58L, or both, were stained with anti-FLAG M2 antibody and Alexa546-labeled secondary antibody. EGFP and Alexa546 fluorescence images were recorded by confocal microscopy. For western blotting, N2A cells were transiently transfected with 3 μg of Cx40 plasmids. Two days after transfection, cells were lysed, and proteins were extracted and separated by conventional methods. Further details are provided in the online-only Data Supplement.

Statistical Analysis

Results are presented as mean±SEM. Mann-Whitney rank sum tests with Bonferroni post hoc correction were used in comparisons for which normality or equal variance assumptions were invalid. In other instances, differences between groups were assessed by 1-way ANOVA followed by Bonferroni post hoc correction. Statistical significance was assumed for $P<0.05$.

Results

Genetic Screening of PFHBI Probands

We genetically screened 156 probands given a clinical diagnosis of PFHBI. We identified 4 novel and 5 previously reported mutations in *SCN5A*,[13,15] 3 mutations in *SCN1B*,[14] and a novel germ line heterozygous missense mutation in exon 2 of the Cx40 gene *GJA5* (online-only Data Supplement Table I). Mutations were not found in connexin genes *GJA1* (Cx43) or *GJC1* (Cx45) or in the other genes screened (*KCNQ1*, *KCNH2*, *KCNE1*, *KCNE2*, *KCNJ2*, *HCN4*, or *SCN4B*). Of the novel *SCN5A* mutations, 1 caused a modification of the amplitude and voltage gating kinetics of the sodium current in heterologously expressing cells (online-only Data Supplement Figure I); 3 other mutant constructs failed to express functional channels, suggesting that patients carrying the mutation were functionally haploinsufficient for Nav1.5 (online-only Data Supplement Figure I). The *GJA5* mutation (c.173A>T) caused an amino acid substitution (glutamine [Q] replaced by leucine [L]) at position 58 in Cx40 (Cx40-Q58L) (Figure 1A and 1B). The mutation was absent in 400 alleles from unaffected control subjects and in the other 155 PFHBI probands. Screening of the entire gene

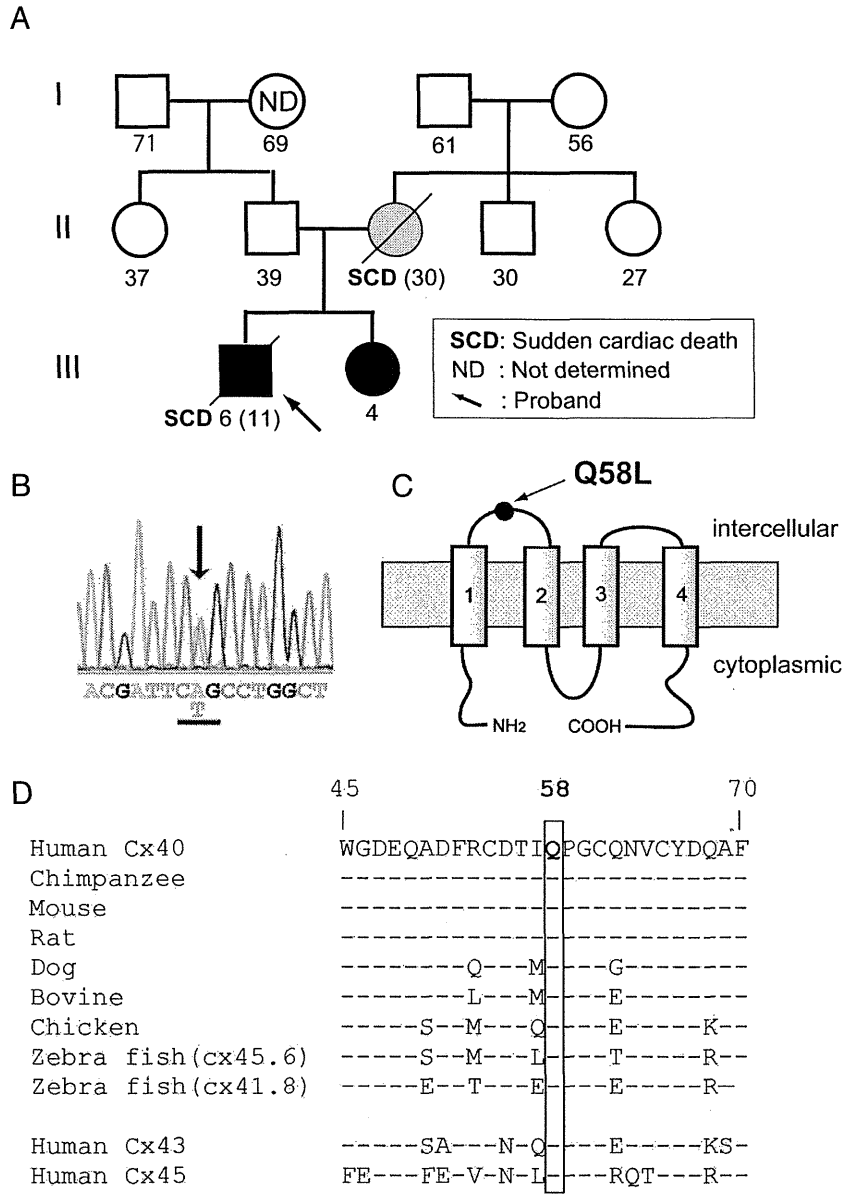

Figure 1. *GJA5* mutation identified in a family given the clinical diagnosis of progressive familial heart block type I. **A,** Family pedigree. Genetically affected and unaffected individuals are shown with closed and open symbols, respectively. The hatched circle indicates the proband's mother not genotyped; clinical data suggest that she was a de novo mutation carrier. Number below each symbol indicates the age at registration or age of SCD (parenthesis). **B,** Sequence electropherogram of exon 2 *GJA5* of proband. Arrow indicates heterozygous missense mutation of leucine (CTG) for glutamine-58 (CAG). **C,** Cx40 predicted membrane topology indicating position Q58 in first extracellular loop. **D,** Sequence alignment of human Cx40 and its homologues (residues 45–70). Notice the conservation in human Cx43 and Cx45. Dashes indicate residues identical with the top sequence. Cx indicates connexin.

panel (including *SCN5A* and *SCN1B*) revealed no other sequence modification in the DNA of this proband. Topological analysis placed amino acid 58 of Cx40 within the first extracellular loop (Figure 1C). The presence of glutamine in this position is highly conserved among *GJA5* orthologs, and 2 other cardiac connexins, Cx43 and Cx45 (Figure 1D). The clinical and genotypic characteristics of proband and tested family members are described next.

Clinical Phenotypes and Genotype of the PFHBI Pedigree With the *GJA5* Mutation

The proband, an 11-year-old boy at time of death, was first referred for evaluation when he was age 6 years because of ECG abnormalities. Although asymptomatic at that time, his ECG showed advanced atrioventricular block, complete left bundle branch block, and left axis deviation (Figure 2A). Echocardiography and cardiac scintigraphy did not reveal signs of structural heart disease. He experienced an episode of syncope at age 9; implantation of a permanent pacemaker was recommended by the physician but not authorized by the legal guardian. The proband died suddenly 2 years later during exercise (running), and the family declined postmortem examination. The proband's younger sister shares the Cx40-Q58L mutation. She is asymptomatic, with a QRS duration at the upper limit of normal, left axis deviation that has been progressive (online-only Data Supplement Table II), and QRS notch. These findings are consistent with impaired intraventricular conduction (Figure 2B). The mother died suddenly at age 30 after delivering the second child. An ECG on record, obtained when she was age 16, was similar to that of the proband (compare Figure 2C with 2A). In addition, a ventricular tachycardia was recorded during the recovery phase of an exercise stress test (online-only Data Supplement Figure II). DNA from the mother was not available for

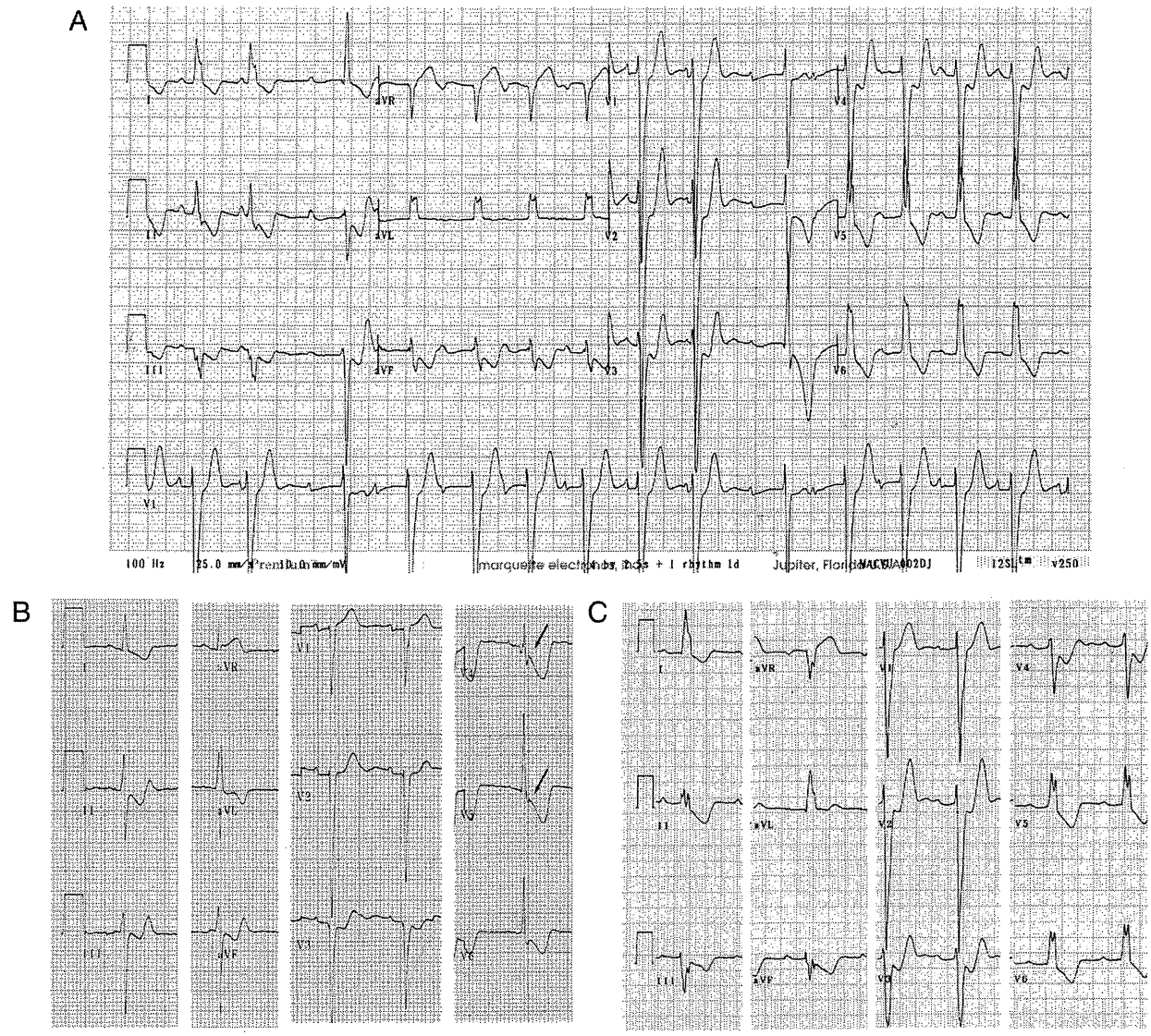

Figure 2. ECGs of proband and affected family members. **A**, ECG of proband at age 6 years, showing advanced atrioventricular block, complete left bundle branch block, and left axis deviation. Patient died suddenly 5 years later. **B**, ECG of proband's sister at age 6 years, showing QRS duration at the upper limit of normal, left axis deviation that has been progressive, and QRS notch in leads V4 and V5 (arrows) consistent with impaired intraventricular conduction. **C**, ECG of proband's mother at age 16 years, showing complete left bundle branch block and left axis deviation. She died suddenly at age 30.

examination. Other family members, including the proband's father, showed normal ECGs. DNA analysis of proband's father and maternal grandparents revealed absence of the Cx40-Q58L mutation. On the basis of clinical data and genotypic features of the proband and sister, it is most likely that the Cx40-Q58L mutation appeared de novo in the proband's mother. The data also indicate an early onset of PFHBI in this family compared with the natural history of the disease in most other cases.[8] As an initial step to assess the functional implications of the Cx40-Q58L mutation, modified constructs were transiently expressed in an exogenous system and evaluated for localization and function.

Electrophysiological Properties of Mutant Cx40-Q58L Channels

Connexin-deficient N2A cells were transiently transfected with cDNA for Cx40-WT or Cx40-Q58L; electrophysiological properties of homologous Cx40 channels were analyzed by conventional dual whole-cell patch clamp. Figure 3A shows representative junctional current traces elicited by a transjunctional voltage gradient of −60 mV. Average junctional conductance (Gj) decreased from 22.2±1.7 nS in cells expressing Cx40-WT (n=14) to 0.56±0.34 nS in cells expressing the Cx40-Q58L mutant (n=14; $P<0.001$). The probability of functional coupling, calculated by dividing the number of electrically coupled pairs by the number of pairs tested, was 100% and 57.1% for Cx40-WT and Cx40-Q58L, respectively.

Figure 3B depicts representative single-channel recordings elicited by a transjunctional voltage of −60 mV in cell pairs expressing Cx40-WT or Cx40-Q58L. Unitary events for WT channels displayed current transitions corresponding to 2 conducting states (O_1 and O_2) of 43.3 and 119.5 pS, respectively. Figure 3C shows the event histograms for both cell

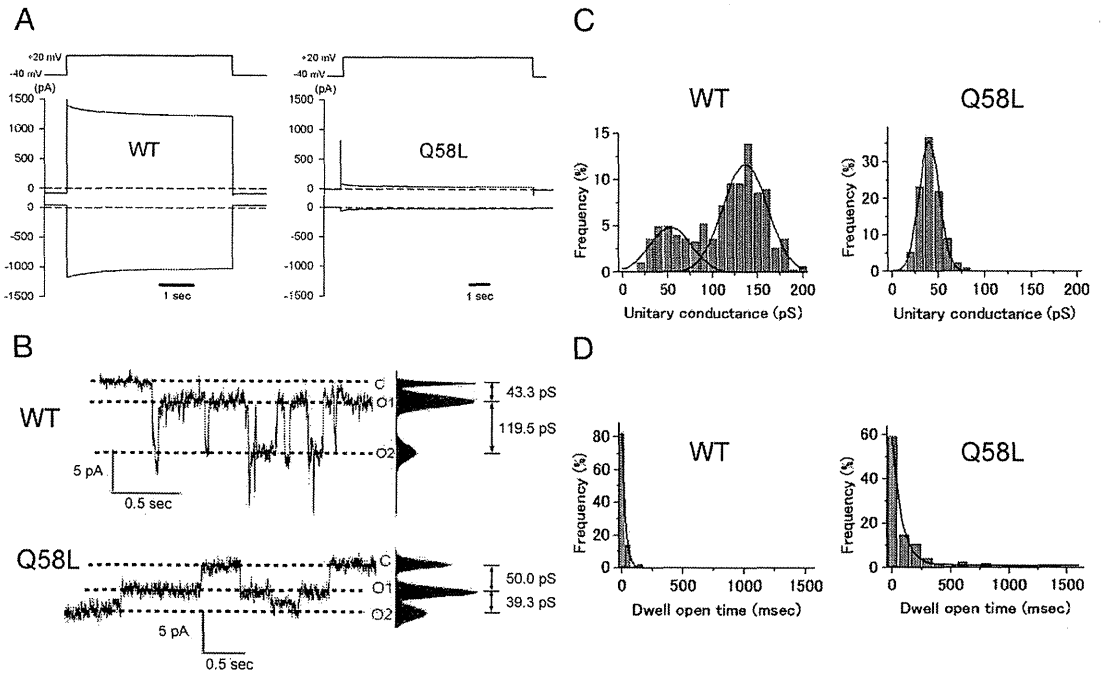

Figure 3. Whole-cell and single-channel properties of connexin40 (Cx40)-WT and Cx40–Q58L channels. **A**, Voltage pulse (top) and junctional current (bottom) from a homomeric WT cell pair (junctional conductance, 12.9 nS) and a Q58L cell pair (junctional conductance, 1.2 nS). **B**, Unitary currents recorded from homomeric Cx40-WT and Cx40–Q58L channels. O_1 and O_2 refer to 2 conducting (open) unitary levels of current. **C**, All-event histograms pooled from WT (n=3) and Q58L (n=3) cells with homologous channels. For WT, Gaussian peaks centered at 136.2±2.3 and 53.1±5.3 pS. For Q58L, best fit by a single Gaussian distribution centered at 40.2±0.3 pS (n=3). **D**, Frequency of events in relation to dwell open time. Binned data were fit by single exponentials (τ_{open} WT, 27.9±0.5 ms, 4 cells, 186 events; τ_{open} Q58L, 92.0±7.8 ms, 3 cells, 163 events). WT indicates wild type.

types (Cx40-WT, 3 cell pairs and 303 events; Cx40-Q58L, 3 cell pairs and 416 events). The histogram for the Cx40-WT channels was best described by 2 Gaussian distributions centered at 136.2±2.3 and 53.1±5.3 pS. In contrast, the histogram for Cx40-Q58L channels was best described by a single Gaussian function centered at 40.2±0.3 pS. Moreover, the length of time that a channel dwelled in the open state (dwell open time) was substantially longer for the Cx40-Q58L channels (92.0±7.8 ms, 3 cell pairs, 163 events) than for Cx40-WT channels (27.9±0.5 ms, 4 cell pairs, and 186 events) (Figure 3D). Of note, the Q58L mutation had a strong dominant effect on formation of heterotypic functional gap junctions. Cells were transfected with either pIRES2-EGFP-Cx40-WT or pIRES2-DsRED2-Cx40-Q58L, and heterotypic pairs were identified by fluorescence microscopy (an EGFP-expressing cell paired with a DsRED2-expressing cell). We recorded from 8 cell pairs and detected unitary current events in only 2 pairs. A total of 57 events were recorded, and average macroscopic junctional conductance was 0.04±0.03 nS. Collectively, the data demonstrated that the Q58L mutation significantly affects the biophysical properties of Cx40 channels and the overall ability of Cx40 gap junctions to form a low-resistance pathway between cells.

Electrophysiological Properties and Gap Junction Plaque Formation in Cells Coexpressing WT and Q58L Proteins

In the clinical cases identified, the Q58L mutation was detected in only 1 carrier allele. Therefore, we assessed the function of gap junctions in cells coexpressing WT and mutant proteins. N2A cells were cotransfected with cDNA for both GFP-tagged Cx40-WT and Cx40-Q58L (0.5 μg of pEGFPN1-Cx40-WT combined with 0.5 μg of pEGFPN1-Cx40-Q58L). Results were compared with those obtained when only 1 of the constructs (1 μg) was transfected. Cells expressing both constructs (WT/Q58L) showed intermediate conductance (15.4±3.7 nS, n=16) between WT (28.8±3.6 nS, n=16, $P<0.001$) and Q58L (0.28±0.11 nS, n=14, $P<0.001$) (Figure 4A). These values were comparable to those obtained using the bicistronic pIRES2-EGFP constructs (WT, 22.2±1.7 nS, n=14; WT/Q58L, 13.0±2.4 nS, n=17; Q58L, 0.56±0.34 nS, n=14). The coexpression results were consistent with those obtained using pIRES plasmids that tagged the cells both green and red, if cotransfected (online-only Data Supplement Figure I). The probability of finding functional coupling in cotransfected cells was 76.5%, which was intermediately between WT (100%) and Q58L (57.1%).

The characteristics of gap junction plaques observed in cells coexpressing WT and Q58L varied significantly between pairs (Figure 4B). Nearly one half of transfected (fluorescence-positive) cells exhibited clear and discrete gap junction plaques (arrow a), whereas the rest of fluorescent-positive cells showed a diffuse expression pattern and absence of well-defined plaques (arrow b). Fluorescence-positive and gap junction plaque-positive cells were counted in 10 different views for each group, and efficacy of gap junction plaque formation was statistically analyzed (Figure 4C) by calculating the ratio of cells with gap junction plaques

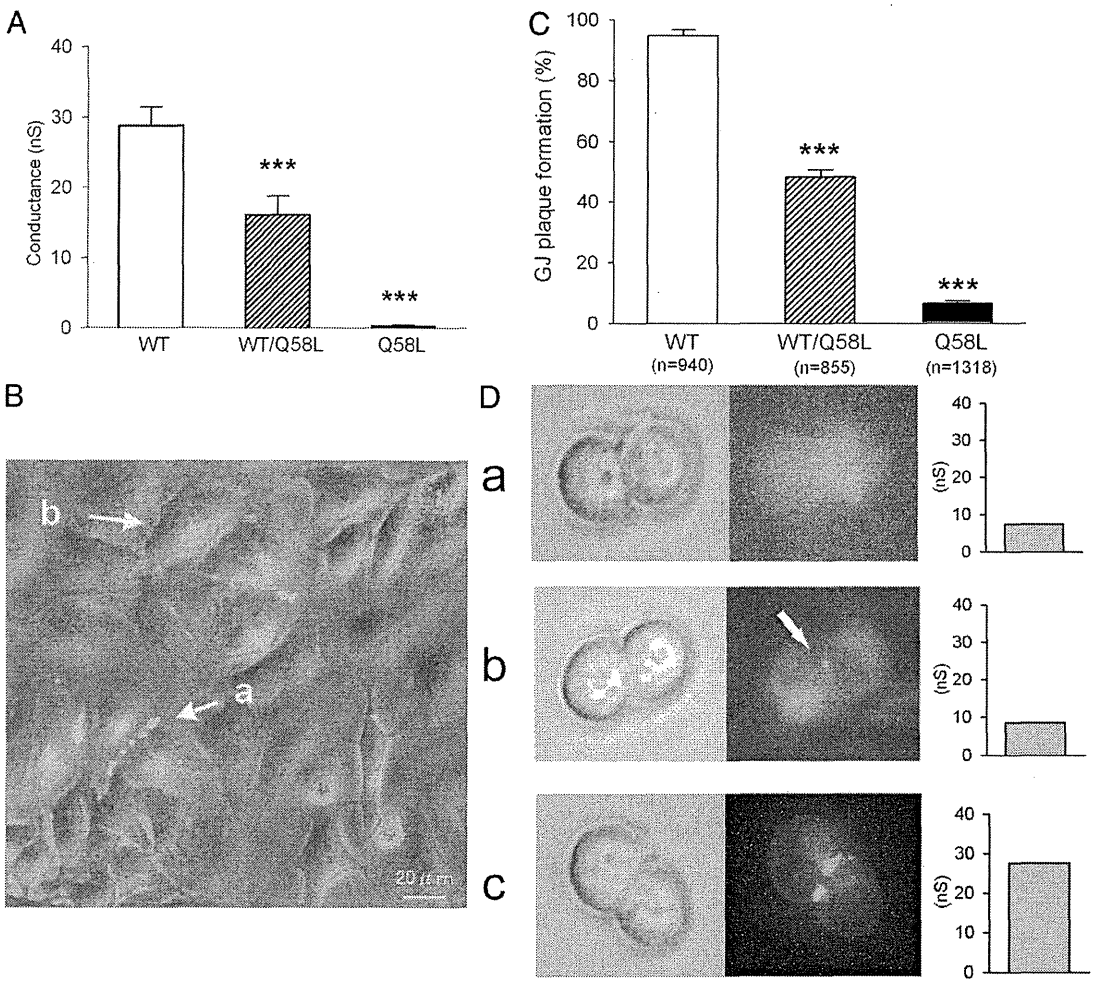

Figure 4. Macroscopic conductance and gap junction plaque morphology in cells coexpressing connexin40 (Cx40)-WT and Cx40-Q58L. **A**, Junctional conductance of cells transfected with plasmid pEGFPN1-Cx40-WT (1 μg), pEGFPN1-Cx40-Q58L (1 μg), or cotransfected with WT and Q58L (WT/Q58L, pEGFPN1-Cx40-WT 0.5μg+pEGFPN1-Cx40-Q58L 0.5 μg). **B**, Phase contrast/fluorescence overlay image of neuroblastoma cells transfected with WT/Q58L constructs. Arrow *a* points to gap junction plaque; arrow *b* points to an example of cells transfected but devoid of gap junction plaque. **C**, Efficacy of gap junction plaque formation was measured as the ratio between the number of gap junction plaque-positive cells and the number of fluorescent-positive cells (WT, n=940; WT/Q58L, n=855; Q58L, n=1318). **D**, Representative images of phase contrast (left), EGFP fluorescence (middle), and junctional conductance (right) from neuroblastoma cells cotransfected with pEGFPN1-Cx40-WT (0.25 μg) and pEGFPN1-Cx40-Q58L (0.25 μg). Three different examples illustrate the relation between plaque morphology and recorded junctional conductance. WT indicates wild type. ***$P<0.001$ compared with WT.

to the number of fluorescence-positive cells. In the Cx40-WT group, almost all fluorescent-positive cells exhibited clear gap junction plaques (94.9±1.9%, n=940), whereas there was a more-diffuse and homogenous pattern with only occasional plaque formation in the Cx40-Q58L group (6.6±0.7%, n=1318, $P<0.001$ compared with WT). In contrast, results varied widely in cells cotransfected with WT/Q58L; nearly one half of fluorescence-positive cells exhibited gap junction plaques similar to those observed in cells transfected with the WT construct (48.2±2.4%, n=855, $P<0.001$), whereas the rest showed a diffuse expression pattern similar to that of Cx40-Q58L. To establish a better correlation between plaque formation and junctional conductance, both variables were measured concurrently in the same cell pair for 39 N2A cell pairs where GFP-tagged plasmids of Cx40-WT and Cx40-Q58L were cotransfected. As shown in Figure 4D, about one half of GFP-positive cell pairs showed a very small Gj (<5 nS) and very few or negligible gap junction plaques (a). In the other half of cell pairs, small, dot-like junctional plaques correlated with intermediate Gj values (b), and there were clear, extensive gap junction plaques associated with Gj values >25 nS (c). Overall, we found significant heterogeneity in the extent of electric coupling, although the measurements of Gj correlated with the localization of proteins in transfected cells. These results indicate that the Q58L mutation significantly impairs the ability of cells to form gap junction plaques, although the effect is not purely dominant when both WT and mutant proteins are coexpressed.

Subcellular Distribution of WT and Q58L Cx40 in Transiently Transfected Cells

To further analyze the subcellular distribution of Cx40-WT and Cx40-Q58L proteins, the C terminal of Cx40-WT was

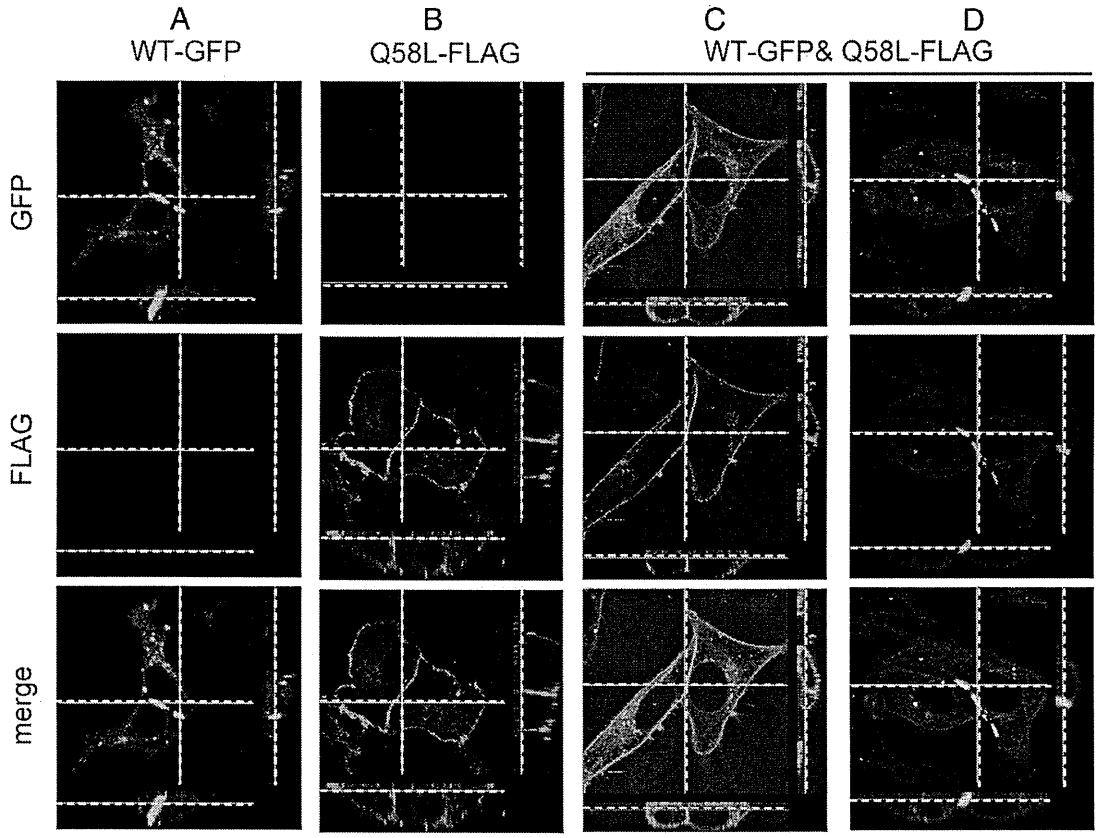

Figure 5. Subcellular distribution of connexin40 (Cx40)-WT and Cx40-Q58L in transiently transfected cells. HeLa cells were transiently transfected with pEGFPN1-Cx40-WT (3.0 μg) (**A**), pCMV-FLAG-Cx40-Q58L (3.0 μg) (**B**), or pEGFPN1-Cx40-WT (1.5 μg) plus pCMV-FLAG-Cx40-Q58L (1.5 μg) (**C**); immunostained for the respective tag protein; and visualized by confocal laser scanning microscopy. Notice that gap junction plaques (**A**) are absent in Q58L transfectants (**B**) and present in some (**D**) but not all (**C**) cotransfected cells. Bar=20 μm. WT indicates wild type.

tagged with GFP, whereas the C terminal of Cx40-Q58L was FLAG tagged. After transfection of N2A cells with the tagged constructs, the distribution of each protein was examined by confocal microscopy. As shown in Figure 5, green color indicates the position of GFP-tagged molecules, whereas red indicates the position of FLAG-tagged molecules. In cells transfected only with GFP-tagged Cx40-WT, fluorescence was consistently detected at sites of cell-cell apposition, following the pattern previously described for GFP-labeled gap junction plaques (Figure 5A). A similar distribution was found when cells were transfected with FLAG-tagged Cx40-WT (not shown). In contrast, most FLAG-tagged Cx40-Q58L signals were evenly distributed around the cell in the vicinity of the plasma membrane (Figure 5B). Biotinylation experiments showed that the Q58L mutation did not prevent the Cx40 protein from inserting into the membrane and presenting a domain-reachable form in the extracellular space (online-only Data Supplement Figure II). Micoscopy experiments in cells coexpressing GFP-tagged Cx40-WT and FLAG-tagged Cx40-Q58L proteins yielded results intermediate to those obtained when only 1 construct was expressed. Nearly one half of cell pairs showed that both proteins distributed homogenously at or near the cell membrane, without the formation of well-defined gap junction plaques (Figure 5C). These images resembled those obtained when only Cx40-Q58L proteins were expressed (Figure 5B, FLAG). In contrast, other cell pairs showed clustering of fluorescent signals within closely confined areas that appeared to be gap junction plaques (Figure 5D).

The experiments described herein led us to speculate that the distribution and function of heteromeric connexons is determined by their mutant subunit content, whereby formation (or not) of plaques and channels are determined, at least in part, by the abundance of expression of one protein over the other. As an initial step to probe this hypothesis, we took advantage of the characteristics of the bicistronic plasmid pIRES, in which the expression rate of the upstream gene is several-fold greater than that of the downstream gene,[20] and explored the functional properties of heteromeric connexons. Cx40-WT and GFP-tagged Cx40-Q58L were subcloned into the pIRES vector, either alone or in combination, in the specific orientations shown in Figure 6A. Protein expression levels of Cx40-WT and Cx40-Q58L were determined by immunochemistry. In contrast to the data obtained when Cx40-WT and GFP-tagged Cx40-Q58L plasmids were cotransfected at a 1:1 ratio (lane 6), expression of heteromeric pIRES plasmids WT-IRES-Q58L-EGFP (lane 3) and Q58L-EGFP-IRES-WT (lane 4) resulted in uneven protein expression levels of WT (40 kDa) and Q58L-EGFP (67 kDa), depending on their orientation in the pIRES vector. Based on

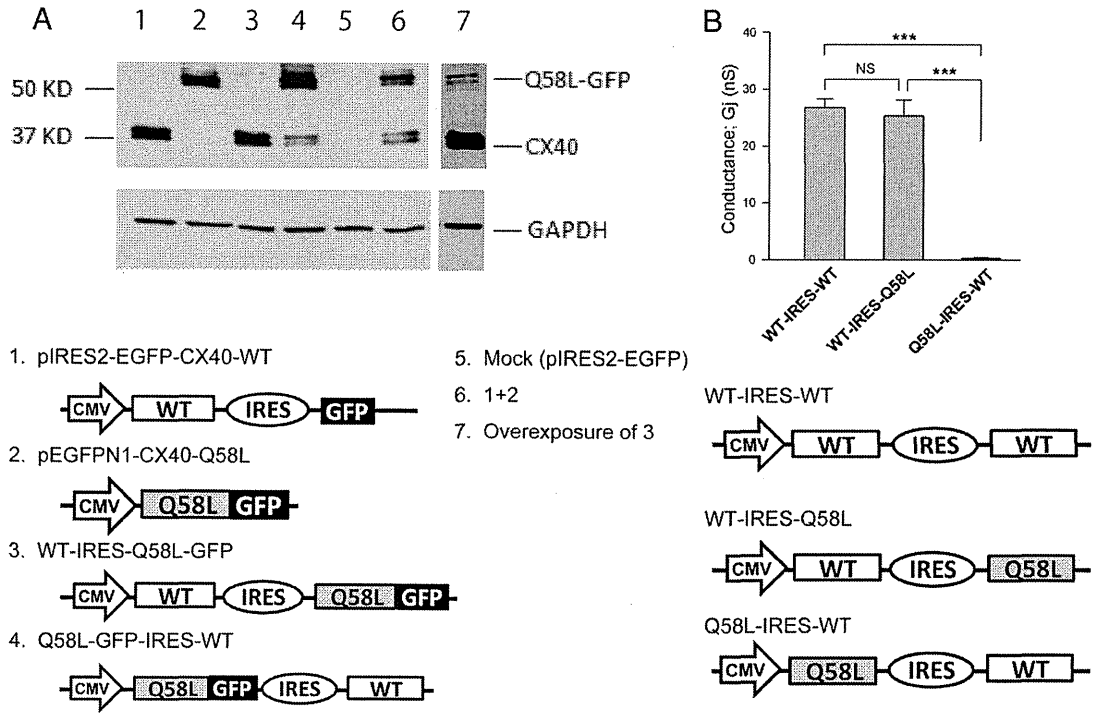

Figure 6. Mutant subunit abundance correlated with gap junction function. **A,** Neuroblastoma cells were transiently transfected with 3 μg Cx40 constructs in IRES plasmids. Cell lysates were analyzed by western blot using anti-Cx40 (top) and anti-GAPDH antibodies (bottom). The number in each lane corresponds to the plasmid noted below the image. Samples from cells cotransfected with plasmids 1 and 2 (1.5 μg each) were loaded on lane 6. Double bands of Cx40-WT (40 kDa) and Q58L-EGFP (67 kDa) are shown in lanes 3, 4, 6, and 7. Results were repeated in 3 separate experiments. Overexposure (lane 7) confirmed expression of the high-molecular-weight protein in lane 3. **B,** Junctional conductance of homomeric and heteromeric constructs (WT-IRES-Q58L and Q58L-IRES-WT). Conductance of cell pairs expressing WT-IRES-WT (n=17) was comparable to heteromeric construct WT-IRES-Q58L (n=17). However, converse heteromeric construct Q58L-IRES-WT (n=15) showed significantly reduced conductance ($P<0.001$ versus WT-IRES-WT and WT-IRES-Q58L). ***$P<0.001$. NS indicates not significant; WT, wild type.

these observations, we constructed a homomeric Cx40-WT plasmid (WT-IRES-WT) and heteromeric plasmids of Cx40-WT and Cx40-Q58L with different orientations (WT-IRES-Q58L and Q58L-IRES-WT) (Figure 6B). The junctional conductance of cell pairs expressing WT-IRES-Q58L (25.3±2.8 nS, n=17) was nearly indistinguishable from that of the homomeric plasmid WT-IRES-WT (27.8±1.4 nS, n=17, *P* not significant). By contrast, the converse heteromeric construct Q58L-IRES-WT showed substantially reduced junctional conductance (0.29±0.12 nS, n=15, $P<0.001$) comparable with that of the homomeric Q58L (0.56±0.34 nS) (Figure 3A). These results suggest that the final electrophysiological properties of the heteromeric connexons are determined predominantly by the numbers of mutant subunits in each gap junction rather than defined by a dominant-negative effect.

Discussion

Genetic screening confirmed the association of *SCN5A* and *SCN1B* with PFHB1[13–15] and revealed novel mutations within these genes (online-only Data Supplement Table I). More importantly, we identified a particularly severe, early onset case of PFHBI associated with a germ line mutation in *GJA5* in 2 blood relatives (proband and sister) given a clinical diagnosis of PFHBI. The data also indicate that the protein expressed (Cx40-Q58L) failed to form functional gap junctions in an exogenous expression system and decreased the probability of gap junction formation in cells coexpressing the WT protein.

So far, *SCN5A*, *SCB1B*, and *TRPM4* are the only genes associated with PFHB1.[11,13,14] The National Human Genome Research Institute database shows no association of *GJA5* single-nucleotide polymorphisms with arrhythmias or conduction system diseases. PR interval and QRS have been associated with several loci, including *SCN5A, SCN10A, NKX2.5,* and *TBX5*[21,22] but not *GJA5*, which is located at chromosome 1q21.1. Overall, the present results suggest that *GJA5* is a candidate gene associated with PFHBI, likely in a small fraction of the affected population. Yet, given the limited cosegregation observed in the reported family, we remain cautious in assigning a causative nature to the *GJA5* mutation. It will be of great interest to expand the screening of *GJA5* at the research level to identify other cases associated with amino acid changes in Cx40, although it may be premature to include *GJA5* as a part of the routine diagnostic screen.[17] The present results also emphasize the importance of Cx40 in the maintenance of normal cardiac rhythm.

To our knowledge, this is the first report of a germ line mutation in Cx40 associated with a high risk of ventricular arrhythmias (online-only Data Supplement Figure II). Other studies have shown somatic mutations of Cx40 or Cx43 in patients with idiopathic atrial fibrillation[5,23]; those mutations

were confined to the atria, and conduction abnormalities in the ventricles or His-Purkinje system were not observed. On the other hand, as in all cases involving identified genetic substrates for disease, the possibility of compound mutations in unexamined genes cannot be excluded. We do emphasize that the mutation led to a severe cellular phenotype in an exogenous expression system, supporting the argument that just the Q58L substitution can impair the formation of gap junctions necessary for propagation of action potentials between cells.

The results show that Cx40-Q58L was abundantly expressed in an exogenous system. The protein reached the vicinity of the cell membrane but failed to form gap junction plaques (Figure 5B). This result may be due to impaired docking of mutant hemichannels within the intercellular space because of the mutation in the extracellular loop (Figure 1C). During trafficking, connexin subunits oligomerize to form a hemichannel (or connexon). Once at the site of cell contact, connexons from apposing cells dock, sealing the hydrophilic path (the channel pore) from the extracellular space. The locking of 2 connexons into 1 gap junction channel is believed to stabilize connexin subunits in place, facilitating aggregation of other oligomers into their vicinity and eventually forming a plaque. Amino acid substitutions within the extracellular loop, as in Q58L, can prevent hemichannel docking and, thus, plaque formation.[24] The present biotinylation experiments indicate that the Q58L protein integrates into the cell membrane, supporting the notion that the inability of the Q58L mutation to form functional gap junctions is related to events that occur after the oligomer is delivered to the cell membrane and before a functional dodecamer converts into a functional channel in a gap junction plaque.

Results obtained in cells coexpressing both mutant and WT proteins clearly show that one subunit can significantly influence the fate of the other (Figure 5). This suggests that Cx40-Q58L subunits retain their ability to oligomerize not only with other mutant subunits, but also with the WT protein. The results also present an interesting paradigm in that neither the WT nor the mutant construct exerted a dominant effect over the other. After transfection with equal amounts of cDNA, we found cells where both WT and mutant proteins displayed the phenotype of the mutant construct, whereas in other cases, junctional plaques could be easily discerned (although an outline of the cell, likely resulting from the presence of the FLAG-tagged mutant protein, could still be observed [see red signal in Figure 5D]). These results can be explained if we assume that the probability of proper targeting and integration of a connexon into a plaque decreases as a function of the number of mutant subunits contained. For cotransfection, we used equal amounts of cDNA; however, it is very likely that each cell was transfected with variable amounts of each construct and, thus, expressed variable amounts of each protein. We speculate that a majority (though of unknown stoichiometry) of WT connexin subunits are required in a connexon for proper formation of functional gap junctions. Thus, if a cell captures an abundance of Q58L cDNA, most oligomers will contain an excess of mutant subunits, and gap junction formation will fail. If, on the other hand, that cell captures and expresses more of the WT cDNA, the distribution of the subunits within the oligomer will contain a majority of WT connexins, and the connexon will be properly integrated into a channel. This hypothesis will require further testing, although data presented in Figure 6 support the concept that success or failure of functional channel formation may relate to relative abundance of each protein (WT or mutant). If our hypothesis is correct, it suggests that the distribution of functional gap junctions in the His-Purkinje network of affected individuals could vary significantly among cells, depending on the extent of expression of each allele in each cell. The resulting phenotype may be that of a Purkinje network where gap junction-mediated coupling could be heterogeneous, setting the stage for local conduction block, microreentry, and ventricular arrhythmias at the Purkinje network or at the Purkinje-muscle junction.[1,2]

Overall, we show that both proband and sister have a genotype that (1) is absent in hundreds of control subjects and in the unaffected parent (the father), (2) disrupts an important functional domain of the protein, and (3) disrupts the formation of gap junction channels. The data therefore support the notion of an association between the Cx40 mutation and the clinical phenotype and emphasize the importance of future studies to assess the possible involvement of Cx40 mutations as causative of the disease.

Acknowledgments

We thank Dr A.L. George for critical reading of the manuscript and Mss M. Fukuoka and C.R. Ingram for technical assistance.

Sources of Funding

This work was supported by research grant 21590921 (to Dr Makita), Scientific Research B (to Dr Mochizuki), and Grant-in-Aid for Scientific Research on Innovative Areas (HD Physiology) 22136007 (to Dr Makita) from the Ministry of Education, Culture, Sports, Science and Technology, Japan; a Health and Labor Sciences Research Grant for research on measures for intractable diseases from the Ministry of Health (2010-145) (to Dr Makita); the Mitsubishi Pharma Research Foundation (to Dr Makita); the Japan-France Integrated Action Program (SAKURA) (to Drs Makita and Schott); The Naito Foundation (to Drs Makita and Seki); the Support Center for Women Health Care Professionals and Researchers 21590921 (to Dr Seki); and grants GM057691, HL106632 and HL087226 from the National Institutes of Health (to Dr Delmar).

Disclosures

None.

References

1. Saffitz JE, Lerner DL, Yamada KA. Gap junction distribution and regulation in the heart. In: Zipes DP, Jalife J, eds. *Cardiac Electrophysiology: From Cell to Bedside.* Philadelphia, PA: Saunders; 2004:181–191.
2. Park DS, Fishman GI. The cardiac conduction system. *Circulation.* 2011; 123:904–915.
3. Ruan Y, Liu N, Priori SG. Sodium channel mutations and arrhythmias. *Nat Rev Cardiol.* 2009;6:337–348.
4. Firouzi M, Ramanna H, Kok B, Jongsma HJ, Koeleman BPC, Doevendans PA, Groenewegen WA, Hauer RNW. Association of human connexin40 gene polymorphisms with atrial vulnerability as a risk factor for idiopathic atrial fibrillation. *Circ Res.* 2004;95:e29–e33.
5. Gollob MH, Jones DL, Krahn AD, Danis L, Gong X-Q, Shao Q, Liu X, Veinot JP, Tang ASL, Stewart AFR, Tesson F, Klein GJ, Yee R, Skanes AC, Guiraudon GM, Ebihara L, Bai D. Somatic mutations in the connexin 40 gene (*GJA5*) in atrial fibrillation. *N Engl J Med.* 2006;354:2677–2688.

6. Lenègre J. Etiology and pathology of bilateral bundle branch block in relation to complete heart block. *Prog Cardiovasc Dis.* 1964;6:409–444.
7. Lev M, Kinare SG, Pick A. The pathogenesis of atrioventricular block in coronary disease. *Circulation.* 1970;42:409–425.
8. Probst V, Kyndt F, Potet F, Trochu JN, Mialet G, Demolombe S, Schott JJ, Baro I, Escande D, Le Marec H. Haploinsufficiency in combination with aging causes SCN5A-linked hereditary Lenègre disease. *J Am Coll Cardiol.* 2003;41:643–652.
9. Brink PA, Ferreira A, Moolman JC, Weymar HW, van der Merwe P-L, Corfield VA. Gene for progressive familial heart block type I maps to chromosome 19q13. *Circulation.* 1995;91:1633–1640.
10. de Meeus A, Stephan E, Debrus S, Jean M-K, Loiselet J, Weissenbach J, Demaille J, Bouvagnet P. An isolated cardiac conduction disease maps to chromosome 19q. *Circ Res.* 1995;77:735–740.
11. Kruse M, Schulze-Bahr E, Corfield V, Beckmann A, Stallmeyer B, Kurtbay G, Ohmert I, Schulze-Bahr E, Brink P, Pongs O. Impaired endocytosis of the ion channel TRPM4 is associated with human progressive familial heart block type I. *J Clin Invest.* 2009;119:2737–2744.
12. Royer A, van Veen TAB, Le Bouter S, Marionneau C, Griol-Charhbili V, Leoni A-L, Steenman M, van Rijen HVM, Demolombe S, Goddard CA, Richer C, Escoubet B, Jarry-Guichard T, Colledge WH, Gros D, de Bakker JMT, Grace AA, Escande D, Charpentier F. Mouse model of SCN5A-linked hereditary Lenègre's disease. Age-related conduction slowing and myocardial fibrosis. *Circulation.* 2005;111:1738–1746.
13. Schott JJ, Alshinawi C, Kyndt F, Probst V, Hoorntje TM, Hulsbeek M, Wilde AA, Escande D, Mannens MM, Le Marec H. Cardiac conduction defects associate with mutations in SCN5A. *Nat Genet.* 1999;23:20–21.
14. Watanabe H, Koopmann TT, Le Scouarnec S, Yang T, Ingram CR, Schott JJ, Demolombe S, Probst V, Anselme F, Escande D, Wiesfeld AC, Pfeufer A, Kaab S, Wichmann HE, Hasdemir C, Aizawa Y, Wilde AA, Roden DM, Bezzina CR. Sodium channel beta1 subunit mutations associated with Brugada syndrome and cardiac conduction disease in humans. *J Clin Invest.* 2008;118:2260–2268.
15. McNair WP, Ku L, Taylor MRG, Fain PR, Dao D, Wolfel E, Mestroni L; Familial Cardiomyopathy Registry Research Group. SCN5A mutation associated with dilated cardiomyopathy, conduction disorder, and arrhythmia. *Circulation.* 2004;110:2163–2167.
16. Miquerol L, Meysen S, Mangoni M, Bois P, van Rijen HVM, Abran P, Jongsma H, Nargeot J, Gros D. Architectural and functional asymmetry of the His-Purkinje system of the murine heart. *Cardiovasc Res.* 2004; 63:77–86.
17. Ackerman MJ, Priori SG, Willems S, Berul C, Brugada R, Calkins H, Camm AJ, Ellinor PT, Gollob M, Hamilton R, Hershberger RE, Judge DP, Le Marec H, McKenna WJ, Schulze-Bahr E, Semsarian C, Towbin JA, Watkins H, Wilde A, Wolpert C, Zipes DP. HRS/EHRA expert consensus statement on the state of genetic testing for the channelopathies and cardiomyopathies. *Heart Rhythm.* 2011;8:1308–1339.
18. Seki A, Coombs W, Taffet SM, Delmar M. Loss of electrical communication, but not plaque formation, after mutations in the cytoplasmic loop of connexin43. *Heart Rhythm.* 2004;1:227–233.
19. Anumonwo JMB, Taffet SM, Gu H, Chanson M, Moreno AP, Delmar M. The carboxyl terminal domain regulates the unitary conductance and voltage dependence of connexin40 gap junction channels. *Circ Res.* 2001;88:666–673.
20. Bochkov YA, Palmenberg AC. Translational efficiency of EMCV IRES in bicistronic vectors is dependent upon IRES sequence and gene location. *Biotechniques.* 2006;41:283–284.
21. Holm H, Gudbjartsson DF, Arnar DO, Thorleifsson G, Thorgeirsson G, Stefansdottir H, Gudjonsson SA, Jonasdottir A, Mathiesen EB, Njolstad I, Nyrnes A, Wilsgaard T, Hald EM, Hveem K, Stoltenberg C, Lochen M-L, Kong A, Thorsteinsdottir U, Stefansson K. Several common variants modulate heart rate, PR interval and QRS duration. *Nat Genet.* 2010;42:117–122.
22. Pfeufer A, van Noord C, Marciante KD, Arking DE, Larson MG, Smith AV, Tarasov KV, Muller M, Sotoodehnia N, Sinner MF, Verwoert GC, Li M, Kao WHL, Kottgen A, Coresh J, Bis JC, Psaty BM, Rice K, Rotter JI, Rivadeneira F, Hofman A, Kors JA, Stricker BHC, Uitterlinden AG, van Duijn CM, Beckmann BM, Sauter W, Gieger C, Lubitz SA, Newton-Cheh C, Wang TJ, Magnani JW, Schnabel RB, Chung MK, Barnard J, Smith JD, Van Wagoner DR, Vasan RS, Aspelund T, Eiriksdottir G, Harris TB, Launer LJ, Najjar SS, Lakatta E, Schlessinger D, Uda M, Abecasis GR, Muller-Myhsok B, Ehret GB, Boerwinkle E, Chakravarti A, Soliman EZ, Lunetta KL, Perz S, Wichmann HE, Meitinger T, Levy D, Gudnason V, Ellinor PT, Sanna S, Kaab S, Witteman JCM, Alonso A, Benjamin EJ, Heckbert SR. Genome-wide association study of PR interval. *Nat Genet.* 2010;42:153–159.
23. Thibodeau IL, Xu J, Li Q, Liu G, Lam K, Veinot JP, Birnie DH, Jones DL, Krahn AD, Lemery R, Nicholson BJ, Gollob MH. Paradigm of genetic mosaicism and lone atrial fibrillation: physiological characterization of a connexin 43-deletion mutant identified from atrial tissue. *Circulation.* 2010;122:236–244.
24. Sosinsky GE, Nicholson BJ. Structural organization of gap junction channels. *Biochim Biophys Acta.* 2005;1711:99–125.

CLINICAL PERSPECTIVE

Progressive familial heart block type I, also known as progressive cardiac conduction defect, is an inherited form of cardiac conduction system dysfunction that can lead to severe heart rhythm disturbances, including sudden cardiac death. The genetic causes of this disease are poorly understood. Here, we genetically screened 156 patients with progressive familial heart block type I. In addition to mutations in genes of the voltage-gated cardiac sodium channel complex (*SCN5A* and *SCN1B*), we found a novel germ line mutation in *GJA5*, the gene encoding the gap junction protein connexin40. The disease had an early onset and was associated with otherwise unexplained sudden cardiac death in the proband and his mother. The proband's sister is also affected. Cellular phenotype analysis revealed impaired gap junction formation at cell-cell interfaces and marked reduction of junctional conductance in cells expressing the mutated connexin40 protein. The results emphasize the importance of connexin40 in normal electrical propagation in the cardiac conduction system and open the possibility of including *GJA5* as a target gene for study in patients with progressive familial heart block type I.

Combined assessment of sex- and mutation-specific information for risk stratification in type 1 long QT syndrome

Jason Costa, MA,* Coeli M. Lopes, PhD,† Alon Barsheshet, MD,* Arthur J. Moss, MD,* Dmitriy Migdalovich, BS,* Gregory Ouellet, MA,* Scott McNitt, MS,* Slava Polonsky, MS,* Jennifer L. Robinson, MS,* Wojciech Zareba, MD, PhD,* Michael J. Ackerman, MD, PhD,‡ Jesaia Benhorin, MD,§ Elizabeth S. Kaufman, MD,‖ Pyotr G. Platonov, MD,¶ Wataru Shimizu, MD, PhD,# Jeffrey A. Towbin, MD,** G. Michael Vincent, MD,†† Arthur A.M. Wilde, MD, PhD,‡‡ Ilan Goldenberg, MD*

*From the *Cardiology Division, University of Rochester Medical Center, Rochester, New York; †Cardiovascular Research Institute, University of Rochester School of Medicine and Dentistry, Rochester, New York; ‡Departments of Medicine, Pediatrics, and Molecular Pharmacology and Experimental Therapeutics, Divisions of Cardiovascular Diseases and Pediatric Cardiology, Mayo Clinic, Rochester, Minnesota; §Department of Cardiology, Tel Aviv Sourasky Medical Center, Tel Aviv, Israel; ‖Heart and Vascular Research Center, MetroHealth Campus of Case Western Reserve University, Cleveland, Ohio; ¶Department of Cardiology, Lund University, Lund, Sweden; #Department of Internal Medicine, Division of Cardiology, National Cardiovascular Center, Suita, Japan; **Department of Pediatrics, University of Cincinnati Children's Hospital, Cincinnati, Ohio; ††LDS Hospital, Salt Lake City, Utah; ‡‡Department of Cardiology, Academic Medical Center, Amsterdam, The Netherlands.*

BACKGROUND Men and women with type 1 long QT syndrome (LQT1) exhibit time-dependent differences in the risk for cardiac events.

OBJECTIVE We hypothesized that sex-specific risk for LQT1 is related to the location and function of the disease-causing mutation in the *KCNQ1* gene.

METHODS The risk for life-threatening cardiac events (comprising aborted cardiac arrest [ACA] or sudden cardiac death [SCD]) from birth through age 40 years was assessed among 1051 individuals with LQT1 (450 men and 601 women) by the location and function of the LQT1-causing mutation (prespecified as mutations in the intracellular domains linking the membrane-spanning segments [ie, S2–S3 and S4–S5 cytoplasmic loops] involved in adrenergic channel regulation vs other mutations).

RESULTS Multivariate analysis showed that during childhood (age group: 0–13 years) men had >2-fold ($P < .003$) increased risk for ACA/SCD than did women, whereas after the onset of adolescence the risk for ACA/SCD was similar between men and women (hazard ratio = 0.89 [$P = .64$]). The presence of cytoplasmic-loop mutations was associated with a 2.7-fold ($P < .001$) increased risk for ACA/SCD among women, but it did not affect the risk among men (hazard ratio 1.37; $P = .26$). Time-dependent syncope was associated with a more pronounced risk-increase among men than among women (hazard ratio 4.73 [$P < .001$] and 2.43 [$P = .02$], respectively), whereas a prolonged corrected QT interval (≥500 ms) was associated with a higher risk among women than among men.

CONCLUSION: Our findings suggest that the combined assessment of clinical and mutation location/functional data can be used to identify sex-specific risk factors for life-threatening events for patients with LQT1.

KEYWORDS: Cytoplasmic-loop mutations; Sex; Long QT syndrome; Sudden cardiac death

ABBREVIATIONS **ACA** = aborted cardiac arrest; **C-loop mutations** = cytoplasmic-loop mutations; **HR** = hazard ratio; **ICD** = implantable cardioverter defibrillator; **LQTS** = long QT syndrome; **LQT1** = long QT syndrome type 1; **MS** = membrane spanning; **QTc** = corrected QT interval; **SCD** = sudden cardiac death

(Heart Rhythm 2012;9:892–898)

Jason Costa, Coeli M. Lopes, Alon Barsheshet, and Ilan Goldenberg contributed equally to this article. This work was supported by research grants HL-33843 and HL-51618 from the National Institutes of Health, Bethesda, MD, and by a research grant from GeneDx to the Heart Research Follow-Up Program in support of the LQTS Registry. Dr Ackerman is a consultant for Transgenomic (approved by Mayo Clinic's Medical-Industry Relations Office and Conflict of Interests Review Board). In addition, "cardiac channel gene screen" and "know-how relating to long QT genetic testing" license agreements, resulting in consideration and royalty payments, were established between Genaissance Pharmaceuticals (then PGxHealth and now Transgenomic) and Mayo Medical Ventures (now Mayo Clinic Health Solutions) in 2004. Dr Ackerman is also a consultant for Biotronik, Boston Scientific Corporation, Medtronic, and St Jude Medical. However, none of these entities provided financial support for this study. **Address reprint requests and correspondence:** Dr Ilan Goldenberg, MD, Heart Research Follow-up Program, Cardiology Division, University of Rochester Medical Center, Box 653, Rochester, NY 14642. E-mail address: Ilan.Goldenberg@heart.rochester.edu.

1547-5271/$ -see front matter doi:10.1016/j.hrthm.2012.01.020

Introduction

Long QT syndrome type 1 (LQT1) is the most commonly occurring of the congenital long QT syndromes (LQTS).[1] It is caused by mutations in the *KCNQ1* gene that impair the slow-acting potassium channel that gives rise to slow delayed rectifier potassium current (I_{Ks}). The resulting prolongation of ventricular repolarization increases the potential for cardiac arrhythmogenic events that can cause syncope or sudden cardiac death (SCD). Patients with LQT1 experience the majority of their events during exercise, possibly because the phase 3 I_{Ks} repolarizing current activates during increased heart rate and is essential for QT-interval adaptation during tachycardia.[1,2] Prior studies have shown that mutations located at the membrane-spanning (MS) region and missense vs nonmissense mutations are associated with a greater risk for cardiac events in patients with LQT1.[3] The MS region includes the MS domains and the MS linkers. Mutations in the intracellular linkers that connect the MS domains of the KCNQ1 (Kv7.1) channel subunit (defined herein as the S2–S3 and S4–S5 cytoplasmic [C]-loop mutations) were shown to affect adrenergic channel regulation by protein kinase A[4] and may therefore predispose to increased risk for life-threatening events in this population.[5]

The phenotypic expression of LQT1 is affected by sex and age, wherein men with LQT1 experience increased risk for cardiac events, mainly during the childhood period.[6] Prior studies, however, did not relate sex-specific risk in this population to the location and function of the disease-causing mutation in the *KCNQ1* gene. Furthermore, sex differences in the clinical course of LQT1 were related previously to a cardiac event composite end point, which comprised mostly nonfatal syncope. Accordingly, the present study was designed to evaluate whether the combined assessment of clinical and mutation location/functional data can identify sex-specific risk factors for life-threatening cardiac events in men and women with LQT1.

Methods

Study population

The study population comprised 1051 LQT1-positive subjects from 259 proband identified families. Patients were drawn from the Rochester, NY, enrolling center (center 1) of the International LQTS Registry (n = 755), the Netherlands LQTS Registry (n = 85), and the Japanese LQTS Registry (n = 83), as well as from data submitted by other investigators specifically for this collaborative mutation analysis project: Denmark (n = 43), Israel (n = 34), Sweden (n = 4), and Salt Lake City, UT (n = 47). The proband in each family had otherwise unexplained, diagnostic corrected QT-interval (QTc) prolongation or experienced LQTS-related symptoms. Patients with congenital deafness were excluded from the study.

Data collection and management

For each patient, information on personal history, including cardiac events, electrocardiograms, and therapies, as well as family history was obtained at enrollment. Clinical data were then collected yearly on prospectively designed forms with information on demographic characteristics, personal and family medical history, electrocardiogram findings, medical therapies, left cardiac sympathetic denervation, implantation of a pacemaker or an implantable cardioverter defibrillator (ICD), and the occurrence of LQT1-related cardiac events. The QT interval was corrected for heart rate (QTc) by using Bazett's formula.[7] Data common to all LQTS registries involving genetically tested individuals were merged electronically into a common database for the present study.

Genotype characterization

The *KCNQ1* mutations were identified with the use of standard genetic tests conducted in academic molecular genetic laboratories including the Functional Genomics Center, University of Rochester Medical Center, Rochester, NY; Baylor College of Medicine, Houston, TX; Windland Smith Rice Sudden Death Genomics Laboratory, Mayo Clinic, Rochester, MN; Boston Children's Hospital, Boston, MA; Laboratory of Molecular Genetics, National Cardiovascular Center, Suita, Japan; Department of Clinical Genetics, Academic Medical Center, Amsterdam, The Netherlands; and Molecular Cardiology Laboratory, Policlinico S. Matteo and University of Pavia, Pavia, Italy.

Mutations were defined as any nonsynonym rare variants (<1% of the healthy population) identified in a proband with a prolonged QT interval. Based on prior data regarding mutation location/function and arrhythmic risk in LQT1,[3–5,8] mutations were categorized by their location and type in the *KCNQ1*-encoded channel subunit as follows: (1) missense mutations in the MS region: defined as amino acid residues from 120 to 355, excluding mutations within the MS linkers; (2) missense mutations in the C loops: defined as the coding sequence involving amino acid residues from 174 to 190 (S2–S3 linker) and from 242 to 259 (S4–S5 linker); (3) missense mutations in the N-terminus region, defined as amino acid residues before 120, and the C-terminus region, defined as amino acid residues after residue 355, were combined into one category labeled as the other region for this analysis (hence called the N/C terminus); and (4) other LQT1 mutations as the reference group (ie, splice sites, in-frame insertions, in-frame deletions, nonsense, and frameshift).

The specific mutations included in the present study, by location, type, and number of patients, are detailed in the Supplementary Appendix Table 1, and the distribution of the mutations in the *KCNQ1* gene by their frequency among study patients is shown in Figure 1.

End point

The primary end point of the study was the occurrence of a first life-threatening cardiac event, comprising aborted cardiac arrest (ACA) (requiring defibrillation as part of resuscitation), or LQT1-related SCD (abrupt in onset without

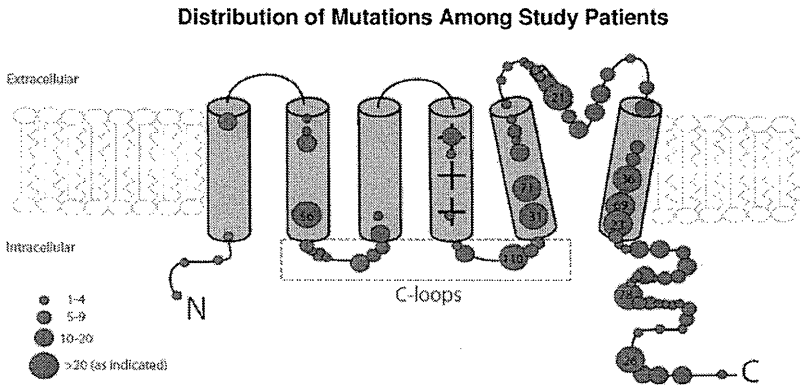

Figure 1 Distribution of mutations in the *KCNQ1* (Kv7.1) potassium channel subunit among study patients. Numbers in larger circles denote the number of patients with the mutation. C loops = cytoplasmic loops.

evident cause, if witnessed, or death that was not explained by any other cause if it occurred in a nonwitnessed setting such as sleep). To further validate the consistency of the results among patients who received an ICD during follow-up, we also assessed a secondary end point comprising the first occurrence of ACA, SCD, or appropriate ICD shock during follow-up.

Statistical analysis

The baseline and follow-up clinical characteristics of the study population were evaluated by using the chi-square test for categorical variables and the Mann-Whitney-Wilcoxon test for continuous variables. The cumulative probability of a first ACA or SCD by sex and by mutation location was assessed by using the Kaplan-Meier method, and significance was tested by using the log-rank test. Follow-up was censored at age 40 years to avoid confounding by acquired cardiovascular disease. Multivariate Cox proportional-hazards regression models were used to evaluate the independent contribution of clinical and genetic factors to the first occurrence of ACA or SCD. Prespecified covariates in the total population model included sex, QTc duration (categorized as a 3-level covariate: >500 ms, 500–550 ms, <500 ms [reference]), mutation location and type (as defined above), the occurrence of syncope during follow-up, and medical therapy with beta-blockers. Syncope and beta-blocker therapy were assessed as time-dependent covariates in the multivariate models. To avoid violation of the proportional hazards assumption due to sex-risk crossover during adolescence, we employed an age-sex interaction term in the total population multivariate model. The effect of each covariate in men and women was assessed by interaction-term analysis (ie, by including a sex-by-risk factor interaction term in the multivariate models), with interactions tested one at a time. Patients without available baseline QTc data (n = 151) were included as a separate (QTc missing) covariate in the multivariate models.

Because almost all the subjects were first- and second-degree relatives of probands, the effect of lack of independence between subjects was evaluated in the Cox model with grouped jackknife estimates for family membership.[9] All grouped jackknife standard errors for the covariate risk factors fell within 3% of those obtained from the unadjusted Cox model, and therefore only the Cox model findings are reported. The statistical software used for the analyses was SAS version 9.20 (SAS Institute Inc, Cary, NC). A 2-sided .05 significance level was used for hypothesis testing.

Results

The clinical characteristics of the study patients by sex are shown in Table 1. Baseline QTc was similar between men and women during childhood and significantly higher among women after the onset of adolescence. During follow-up, similar numbers of men and women were treated with beta-blockers, but a higher proportion of women were treated with an ICD. There were no significant sex differences in the distribution of the mutation by location (Table 1). However, patients with missense mutations localizing to the C loops exhibited a significantly longer baseline QTc (503 ± 58 ms) than did patients with other mutations (480 ± 51 ms; $P <$ .001).

Risk factors for ACA or SCD in the total LQT1 population

During follow-up, 138 study patients (13%) experienced the primary end point of a first ACA or SCD. Kaplan-Meier event rates were significantly higher among men than among women throughout follow-up (P = .008 for the overall difference; Figure 2). Notably, life-threatening cardiac events among men occurred predominantly during childhood, whereas among women event rates increased after this time period. Thus, by age 14 years, the cumulative probability of ACA or SCD was 10% among men as compared with only 3% among women, and by age 40 years, the respective events rates were 19% and 15% (Figure 2).

Consistent with those findings, multivariate analysis in the total study population showed that during childhood men had >2-fold (P = .003) increase in the risk for ACA or SCD as compared with women whereas after the onset of adolescence, there was no statistically significant difference in the risk for ACA or SCD between men and women (hazard ratio [HR] 0.89; P = .64; Table 2). Additional risk

Table 1 Characteristics of the study population

Characteristic	Men (n = 450)	Women (n = 601)	P
ECG parameters			
Overall QTc (ms)	473 ± 55	486 ± 55	<.001
Age ≤ 13 y	486 ± 53	485 ± 54	.21
Age > 13 y	460 ± 53	487 ± 56	<.001
QTc > 500 ms (%)	22	27	.09
RR (ms)	842 ± 220	837 ± 199	.55
Mutation location (%)			
Cytoplasmic loop (S2–S3 or S4–S5 linkers)	19	19	.92
MS	53	54	.67
N/C terminus	28	26	.58
Mutation type (%)			
Missense	83	79	.13
LQTS therapies during follow-up (%)			
Beta-blockers	45	46	.74
Pacemaker	1.6	1.5	.94
ICD	4	9	.003
LCSD	1.1	0.5	.30
Cardiac events during follow-up (%)			
Syncope	35	36	.84
ACA	3	4	.22
SCD	13	8	.007
Appropriate ICD shocks	0.2	1.7	.03
ACA or SCD*	15	11	.07

Values are mean ± SD unless otherwise indicated.

ACA = aborted cardiac arrest; ECG = electrocardiogram; ICD = implantable cardioverter defibrillator; LCSD = left cervical sympathetic denervation; LQTS = long QT syndrome; MS = membrane spanning; QTc = corrected QT interval; SCD = sudden cardiac death; SD = standard deviation.

*Only the first event for each patient was considered.

factors within the total study population included the presence of missense mutations localizing to the C loops (1.9-fold risk increase [$P = .005$]), QTc 500–550 and >550 ms (>3-fold and >4-fold risk increase, respectively [$P < .001$ for both]), and the occurrence of syncope during follow-up (3.4-fold risk increase [$P < .001$]; Table 2). Results were similar when the secondary end point of a first ACA, SCD, or appropriate ICD shock was assessed.

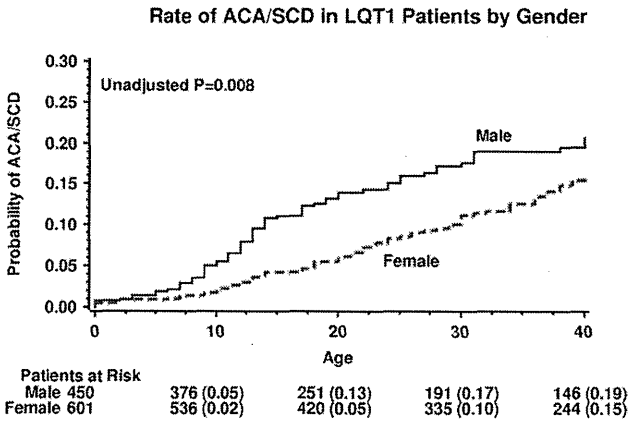

Figure 2 Kaplan-Meier estimates of the cumulative probability of aborted cardiac arrest or sudden cardiac death in patients with LQT1 by sex. ACA = aborted cardiac arrest; LQT1 = long QT syndrome type 1; SCD = sudden cardiac death.

Table 2 Multivariate analysis: Risk factors for ACA/SCD among all patients with LQT1*

Risk factor	Relative risk: Hazard ratio	95% Confidence interval	P
Sex			
Men vs women ≤ 13 y	2.31	1.41–3.92	.003
Men vs women >13 y	0.92	0.61–1.51	.72
Mutation location (vs nonmissense mutations)			
Cytoplasmic loop (S2–S3/S4–S5 linkers)	1.93	1.37–2.75	.005
MS (S1, S2, S3, S4, S5, P-loop, S6)	1.02	0.71–1.85	.51
N/C terminus	0.96	0.52–1.57	.72
QTc duration (ms)			
>550 vs <500	4.18	2.06–8.46	<.001
500–550 vs <500	3.35	1.83–6.11	<.001
Time-dependent syncope			
Syncope vs no syncope	3.40	2.22–5.21	<.001

ACA = aborted cardiac arrest; LQT1 = long QT syndrome type 1; MS = membrane spanning; QTc = corrected QT interval; SCD = sudden cardiac death.

*Models were further adjusted for missing QTc values, time-dependent beta-blocker therapy.

Sex-specific risk factors for life-threatening cardiac events in patients with LQT1

Kaplan-Meier survival analysis showed that women with LQT1 with missense C-loop mutations exhibited a significantly higher rate of ACA or SCD than did women whose LQT1-causative mutation localized elsewhere ($P < .001$ for the overall difference during follow-up; Figure 3A). In contrast, among men, the respective rates of ACA or SCD remained high, predominantly during the childhood period, regardless of mutation location/type ($P = .33$ for the overall difference during follow-up [Figure 3B]).

Sex-specific multivariate analysis (Table 3) showed that women with C-loop mutations exhibited nearly a 3-fold ($P = .01$) increased risk for ACA or SCD than did women with other mutation types, whereas the risk for ACA or SCD among men was not significantly different by mutation location/type (P value for mutation-location-by-sex interaction = .07). Similar results were observed in an additional analysis in which the large subset of patients with the V254M C-loop mutation was excluded from the multivariate models (risk associated with C loop vs other mutations among women: HR 2.55, 95% confidence interval [CI] 1.02–5.94; among men: HR 1.03, 95% CI 0.33–4.11).

Additional risk factors for ACA or SCD among both men and women included a prolonged QTc and the occurrence of

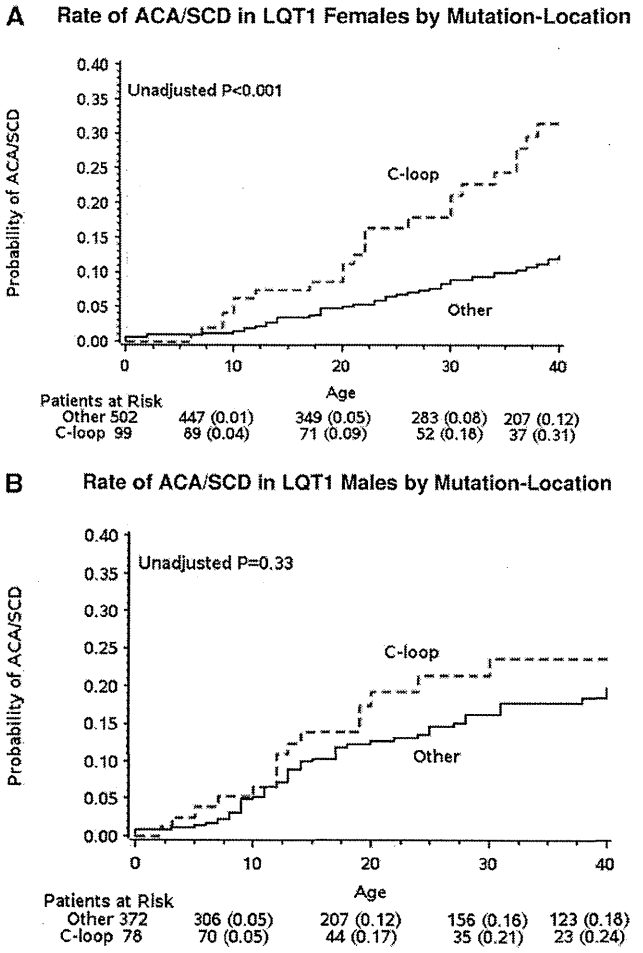

Figure 3 Kaplan-Meier estimates of the cumulative probability of aborted cardiac arrest or sudden cardiac death in **(A)** women with LQT1 and **(B)** men with LQT1, by mutation location. ACA = aborted cardiac arrest; C-loop mutations = cytoplasmic-loop mutations; LQT1 = long QT syndrome type 1; SCD = sudden cardiac death.

time-dependent syncope (Table 3). Notably, women with prolonged QTc, both in the range of 500–550 ms and >550 ms, experienced a pronounced increase (approximately 6-fold) in the risk of ACA or SCD, whereas the risk associated with a prolonged QTc in men was more modest and evident only in those with QTc >550 ms (Table 3 and Figures 4A and B, respectively). The occurrence of syncope during follow-up was associated with a 4-fold ($P < .001$) increase in the risk for subsequent ACA or SCD among men and with a 2.4-fold ($P = .002$) increase in the risk for subsequent ACA or SCD among women.

The combined assessment of clinical and genetic data identified a very low rate of life-threatening events (0.03 events per 100 patient-years) among women aged 13 years or younger without C-loop mutations, no history of prior syncope, and QTc <500 ms.

Time-dependent medical therapy with beta-blockers was associated with a significant 61% reduction in the risk for ACA or SCD in the total study population (HR 0.39; 95% CI 0.22–0.70; $P = .001$), with beta-blocker protection seen similarly between men and women (P values for beta-blocker-by-sex interaction = .56). Notably, this analysis showed that the risk associated with C-loop mutations in women was even more pronounced among those who did not receive beta-blocker therapy (HR 4.51; 95% CI 2.57–7.23; $P < .001$).

Discussion

In the present study, we assessed for the first time sex-specific risk factors for life-threatening cardiac events in a large population of 1051 genetically confirmed patients with LQT1. Our findings show that among probands and relatives with LQT1, (1) men exhibit a significantly higher rate of life-threatening cardiac events than do women, especially prior to puberty, and (2) mutation location shows a sex-specific association with the risk for ACA or SCD. Thus, the risk for life-threatening events was shown to be increased among women with LQT1 with mutations localizing to C-loop domains (S2–S3 and S4–S5) of the *KCNQ1*-encoded protein, whereas the risk for ACA or SCD among men with LQT1 was high even among those who harbored mutations localizing to other regions of the channel that had been ascribed previously as lower-risk mutations. These findings suggest that a combined approach that incorporates clinical and genetic data can be used for improved risk assessment and management of men and women with LQT1.

A previous study from the International LQTS Registry has shown that men with LQT1 have an increase in the risk for any LQT1-related cardiac event, including syncope, during childhood, whereas after the onset of adolescence the risk for events in this population is attenuated without a significant sex difference.[6] Because of a limited sample of 243 patients with LQT1, the study did not assess sex-related differences in the risk for only life-threatening cardiac events (ACA or SCD) in this population. Thus, our findings of the present study extend prior observations and show that men with LQT1 display a higher rate of ACA or SCD than do women from birth through age 40 years, with a predominant risk increase during the childhood period.

Patients with LQT1 experience ventricular tachyarrhythmias more frequently during physical effort,[2] possibly due to the lack of adaptive QT shortening with decreasing RR intervals during tachycardia.[10] Thus, the early predominance of life-threatening cardiac events among men may be related to sex differences in the level of physical activity during childhood among registry patients. After the onset of adolescence, an increase in the levels of testosterone, which was shown to shorten action potential duration and ventricular repolarization,[11–13] may result in a reduction in the risk for arrhythmic events in men. This mechanism is supported by the fact that the risk for life-threatening events during childhood was higher among men despite the fact that the average QTc was similar between men and women during this time period, whereas after the onset of adolescence the QTc was significantly reduced in men and remained virtually unchanged in women (Table 1).

Table 3 Multivariate analysis: Risk factors for ACA/SCD among patients with LQT1 by sex*†

	Men with LQT1		Women with LQT1	
	HR (95% CI)	*P*	HR (95% CI)	*P*
Mutation location (vs nonmissense mutations)				
Cytoplasmic loop (S2–S3/S4–S5 linkers)	1.21 (0.72–2.04	0.48	2.62 (1.59–4.26)	<.001
MS	1.02 (0.63–1.97)	0.54	1.01 (0.62–1.89)	.56
N/C terminus	0.89 (0.52–1.91)	0.87	1.14 (0.51–2.37)	.43
QTc duration (ms)				
500–550 vs <500	1.70 (0.63–4.57)	0.29	6.85 (2.74–17.10)	<.001
>550 vs < 500	3.11 (1.19–8.15)	0.02	5.93 (1.89–18.62)	.002
Time-dependent syncope				
Syncope vs no syncope	4.06 (2.22–7.41)	<0.001	2.43 (1.43–4.85)	.002

ACA = aborted cardiac arrest; CI = confidence interval; HR = hazard ratio; LQT1 = long QT syndrome type 1; QTc = corrected QT interval; SCD = sudden cardiac death; MS = membrane spanning.

*Findings were further adjusted for missing QTc values, time-dependent beta-blocker therapy.

†Models were carried out in the total population by using interaction-term analysis, with interactions tested one at a time; cytoplasmic loop-by-sex interaction = .07; all other interaction *P* values were >.10.

Mutations located in the MS region, including the MS domains and the C loops, of the KCNQ1 protein have been associated with greater prolongation in the QTc during exercise[14] and an increase in the risk for cardiac events in patients with LQT1.[3] Importantly, the C loops were shown to modify the function of KCNQ1 channel subunit, including functional interaction with the auxiliary beta subunits encoded by KCNE1 and modulation of the channel's protein kinase A (PKA)-dependent, adrenergic regulation.[4] Thus, patients who harbor C-loop mutations may be sensitive to even mild degrees of adrenergic stimulation, resulting in arrhythmic events that may occur during less intense physical activity. This mechanism may explain the sex-specific association of mutation location to arrhythmic risk shown in the present study, as women who carry mutations in the adrenergic-sensitive C loops may have an increased risk for life-threatening events even during milder degrees of physical activity. In contrast, participation in more intense physical activity among men with LQT1, especially during childhood, may predispose them to arrhythmic events even among those who carry non–C-loop mutations (which are less sensitive to sympathetic activation). It is also possible that sex differences in the regulation of the ion channel contribute to the differential effect of mutation location/function on arrhythmic risk between men and women.

Similar to prior studies,[15–17] we have also shown that QTc is a major risk factor for cardiac events in patients with LQTS. However, our data suggest that in LQT1 the risk associated with QTc is more pronounced among women (who exhibited >6-fold risk with QTc exceeding 500 ms, whereas a significant risk increase among men was evident only among those with QTc >550 ms).

It was suggested recently that patients with LQT1 experience a very low rate of cardiac events during beta-blocker therapy.[18] In the present study, medical therapy with beta-blockers was associated with a pronounced reduction in the risk for ACA or SCD in the total LQT1 population, without a statistically significant difference between men and women. However, our findings suggest that sex-specific risk factors should be taken into account in the management of patients with LQT1. These clinical and mutation-related risk factors are shown in Figure 1 of the Supplementary Appendix and include (1) the preadolescence period in men, especially among those who experience syncope during childhood and those with QTc >550 ms, and (2) following the onset of adolescence in women, especially among those with C-loop mutations, QTc ≥500 ms, and/or history of syncope.

Study limitations

Although we have shown recently that the S2–S3 and S4–S5 C-loop linkers have an important functional role in adrenergic channel regulation through PKA,[4,5] further studies are needed to relate the functional expression of discrete *KCNQ1* mutations to sex-specific risk in LQT1, and their interaction with possible hormonal modulation of cardiac risk in this population.

The present study shows that beta-blocker therapy is associated with a significant reduction in the risk for life-threatening events in both men and women with LQT1. However, because of sample size limitations, we did not evaluate sex-specific differences in response to beta-blocker therapy between patients with LQT1 with higher-risk (and adrenergic-sensitive) C-loop mutations and those with mutations localizing elsewhere. In addition, we did not carry out comprehensive analysis of the relationship between all functional regions of the *KCNQ1*-encoded protein (including functional areas within the C-terminus or N-terminus domains) and sex-specific risk.

We excluded patients with congenital deafness from the study. However, 12 patients (1%) had 2 different mutations in the *KCNQ1* gene. To validate the consistency of the results for patients with single mutations, all multivariate models were repeated after excluding the 12 patients with >1 mutation. This confirmatory analysis yielded virtually identical results regarding the risk associated with clinical factors and mutation location as in the primary analysis.